

AD-A064 047 AIR FORCE INST OF TECH WRIGHT-PATTERSON AFB OHIO SCH--ETC F/G 17/7
ERROR MODEL VERIFICATION FOR A THREE AXIS LASER GYRO STRAPDOWN --ETC(U)
DEC 78 R S LAWRENCE

UNCLASSIFIED

AFIT/GGC/EE/78-8

NL

1 OF 2
AD
A064 047





AFIT/GGC/EE/78-8

LEVEL II

AD A064047

DDC FILE COPY.

⑨ Master's thesis,

6
ERROR MODEL VERIFICATION

FOR A

THREE AXIS LASER GYRO
STRAPDOWN INERTIAL MEASUREMENT UNIT.

THESIS

⑭ AFIT/GGC/EE/78-8 ⑯ Robert S. Lawrence
Capt USAF

DDC

REF ID: A64047

JAN 31 1979

⑮ Dec 78

⑯ 98p.

APPROVED
SOLVED
A

Approved for public release; distribution unlimited

012225

503

79 01 30 147

ERROR MODEL VERIFICATION FOR A THREE AXIS LASER GYRO
STRAPDOWN INERTIAL MEASUREMENT UNIT

THESIS

Presented to the Faculty of the School of Engineering
of the Air Force Institute of Technology
Air Training Command
in Partial Fulfillment of the
Requirements for the Degree of
Masters of Science

by

Robert S. Lawrence, BSE
Capt USAF

Graduate Guidance and Control
December 1978



Approved for public release; distribution unlimited.

Preface

The introduction of the laser gyroscope has provided the characteristics needed for further development of strapdown inertial navigation systems. This design project represents a very straight-forward and inexpensive application of obtaining digital data from a laser gyroscope strapdown inertial measurement unit for error analysis. Since it was my first experience with laser gyros and a strapdown system, it represents a very gratifying and educational experience.

In this thesis, I tried to explain the operations of the IMU, the designed interface equipment, and an application of the data obtained from the IMU. I have also provided detailed schematic diagrams of the designed interface equipment and a descriptive computer listing to aid other users.

I would like to acknowledge the help and guidance of my thesis advisor, Major Salvatore Balsamo, and the advice of Dr. Gary Lamont in overcoming many problems. I would also like to thank Mr. Robert Durham of the Department of Electrical Engineering Laboratory for his support in the laboratory set-up. I also wish to acknowledge my indebtedness to my wife for her assistance in the preparation of this report.

Robert S. Lawrence

Contents

	Page
Preface.....	ii
List of Figures.....	v
List of Tables.....	vii
Abstract.....	viii
I. Introduction.....	1
Background.....	1
Purpose.....	2
Scope.....	2
II. Inertial Measurement Unit Characterisites.....	4
General Description.....	4
Sensor Assembly.....	4
Electronic Assembly.....	9
III. Laboratory Test Set-Up.....	12
System Description.....	12
Equipment Description.....	14
IMU/Digital Computer Interface.....	14
Data Monitor Controller.....	18
Multiplexer.....	20
Programmer.....	25
Test Fixture.....	29
IV. Test Data Processing.....	32
Computer Program Description.....	32
Typical Test Data.....	35
V. Calibration Test.....	41
Model Equation.....	41
Static 6-Position Test.....	42
Test Description.....	42
Test Procedure.....	44
Dynamic 6-Position Test.....	47
Test Description.....	47
Test Procedure.....	48
Data Analysis.....	48
VI. Results and Recommendations.....	57

Contents

	<u>Page</u>
Results.....	57
Recommendations.....	58
Bibliography.....	62
Appendix A: Schematic Diagrams and Parts List.....	63
Appendix B: Computer Program Listing.....	78

List of Figures

Figure		Page
II-1	IMU Functional Block Diagram.....	5
II-2	Laser Gyro Optical Schematic(Ref 1).....	6
II-3	Accelerometer Exploded View(Ref 6).....	10
III-1	Block Diagram of the Laboratory Test Set-Up....	13
III-2	IMU/Computer Interface Block Diagram.....	15
III-3	IMU/Computer Timing Diagram.....	17
III-4	Data Monitor Controller Block Diagram.....	19
III-5	Data Monitor Controller Signals.....	22
III-6	Multiplexer Block Diagram.....	24
III-7	Decoder Signals.....	23
III-8	Multiplexer Signals.....	26
III-9	Programmer Block Diagram.....	28
III-10	Programmer Signals.....	30
III-11	Sensor Assembly Test Fixture.....	31
IV-1	Program Major Steps Flowchart.....	33
IV-2	Detailed Program Flowchart.....	36
V-1	IMU Sensitive Axes Orientation(Ref 1).....	43
V-2	Accelerometers Reference Position.....	42
V-3	Accelerometer Calibration Positions.....	45
V-4	Gyros Reference Position.....	47
V-5	Gyro Calibration Positions.....	49
V-6	Accelerometer Standard Deviation vs. Integration Time.....	52
V-7	Gyro Standard Deviation vs. Integration Time....	53
V-8	Gyro Scale Factor Error vs. Rotation Rate.....	56

List of Figures

Figure		Page
A-1	Data Monitor Controller Schematic 1 of 2.....	64
A-2	Data Monitor Controller Schematic 2 of 2.....	65
A-3	Multiplexer Schematic(Decoder) 1 of 6.....	66
A-4	Multiplexer Schematic(Buffer Group#1) 2 of 6....	67
A-5	Multiplexer Schematic(Buffer Group#2) 3 of 6....	68
A-6	Multiplexer Schematic(Mux Group#1) 4 of 6.....	69
A-7	Multiplexer Schematic(Mux Group#2) 5 of 6.....	70
A-8	Multiplexer Schematic(Binary Counter) 6 of 6....	71
A-9	Programmer Schematic.....	72

List of Tables

Table	Page
III-I Test Words Chart.....	21
IV-I Typical Test Data.....	40
V-I Accelerometer Calibration Equations.....	46
V-II Gyro Calibration Equations.....	50
VI-I Accelerometer(Static) Test Data.....	60
VI-II Accelerometer Calibration Equation Solutions....	61
A-I Data Monitor Controller Parts Listing.....	73
A-II Multiplexer Parts Listing.....	75
A-III Programmer Parts Listing.....	77

Abstract

↓ A digital data acquisition system was developed to obtain data from a Sperry laser gyroscope strapdown inertial measurement unit for error model verification. The system consisted of a laboratory test set-up with the inertial measurement unit (IMU) on the Genisco rate table and input/output interfaces such that meaningful IMU sensor data was recorded on magnetic tape with absence of a microprocessor. The recorded data was processed on the CDC 6600 digital computer by a specially developed program which formats the data in accordance to desired specifications. The calibration sequence for error model verification was a 6-position dynamic test for the laser gyros and a 6-position static test for the accelerometers. The result is a reliable and flexible system that can obtain data from the IMU in the laboratory for analysis.

↑

ERROR MODEL VERIFICATION FOR A THREE AXIS LASER GYRO
STRAPDOWN INERTIAL MEASUREMENT UNIT

I. Introduction

Background

The strapdown inertial measurement unit under consideration in this thesis project is a self-contained assembly designed to sense incremental displacement about its axes and velocity increments along the axes and transmit these signals in the form of discrete pulses to a digital computer in order to perform the function of:

1. Calibration and/or alignment
2. Navigation
3. Guidance

The system is mechanized by mounting three gyros and three accelerometers solidly onto the main frame of the vehicle in which it is used. One of the most promising and serious competitors to the conventional spinning-mass mechanical gyroscope for measuring angular rotation rates in the strapdown configuration is the laser gyroscope. This gyro has a number of desired characteristics, such as performance being unaffected by high-g environment, the absence of rotating parts, and rapid turn-on time. Also the laser gyroscope can provide the characteristics needed for further development and exploitation of strapdown systems, particularly for applications which demand high rotation rates.

Sperry Gyroscope which developed the first laser gyro,

built a strapdown laser gyroscope inertial measurement unit that permits three laser gyros, with their sensitive axes orthogonally oriented, to be fabricated in a single cluster. This IMU (Part number 4331-70492) contains three Sperry model SLG-15 Laser gyros and three Sundstrand Q-flex accelerometers, which is experimentally set up to be evaluated in this thesis.

Purpose

The purpose of this work is an experimental verification of an error model for the Sperry strapdown inertial measurement unit. An extensive effort was necessary initially to set-up the inertial measurement unit (IMU) on the Genisco rate table and design the required input/output interfaces such that meaningful IMU sensor data can be recorded on magnetic tape. A detailed calibration sequence was developed and a series of test executed to obtain the required data. This data will be utilized to determine the coefficients of the models developed for the calibration sequence.

Scope

This report contains six chapters. Chapter II is a description of the Sperry strapdown IMU used in the experiment. Chapter III contains the laboratory test set-up with descriptions of the equipment designed to interface the IMU to the magnetic tape recorder. Chapter IV gives a description of the FORTRAN computer program to process the recorded test data on a digital computer. Chapter V is a description of the calibra-

tion test and data analysis developed for the gyros and accelerometers. Chapter VI contains results and recommendations.

Appendix A includes schematic diagrams of designed interface equipment. Appendix B is a listing of the computer program to process the recorded data tapes.

II. Inertial Measurement Unit Characteristics

General Description (Ref 1:1)

The Sperry strapdown laser gyro inertial measurement unit (IMU) consists of two separate assemblies; a sensor assembly and an electronics assembly as shown in Figure II-1. The sensor assembly contains three Sperry model SLG-15 laser gyros and three Sundstrand Q-Flex accelerometers mounted on a common orthogonal structural element. The electronics assembly contains the electronics modules necessary for laser gyro control and signal processing, accelerometer signal processing and a custom interface module to accommodate IMU interfacing with a system digital computer.

Sensor Assembly (Ref 1:14-18)

The sensor assembly which contains the gyros and accelerometers are in a unique integrated design. The three laser gyros are machined into a single block (optical cavity) of CER-VIT (low expansion ceramic vitreous material) so that their optical paths are interwoven. The three force rebalanced accelerometers are also mounted on the optical cavity. The optical cavity is mounted in an evacuated case and protected by a multi-layer magnetic shield.

The three gyros are identical. Figure II-2 is an optical schematic diagram of the laser gyro. The gyro optical path is approximately an equilateral triangle, five inches on a side, defined by three mirrors. The gyro input axis is normal to

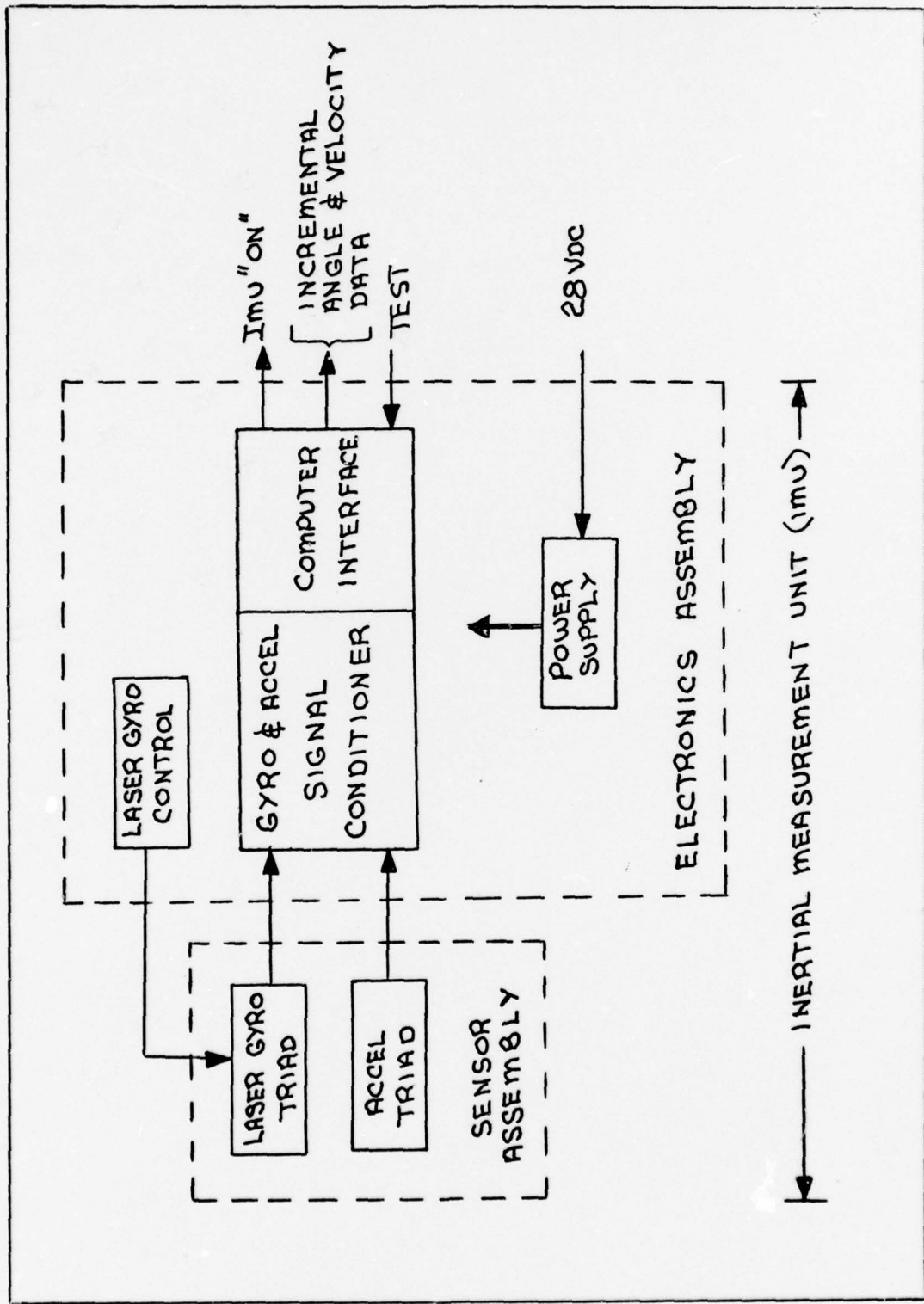


Figure II-1. IMU Functional Block Diagram

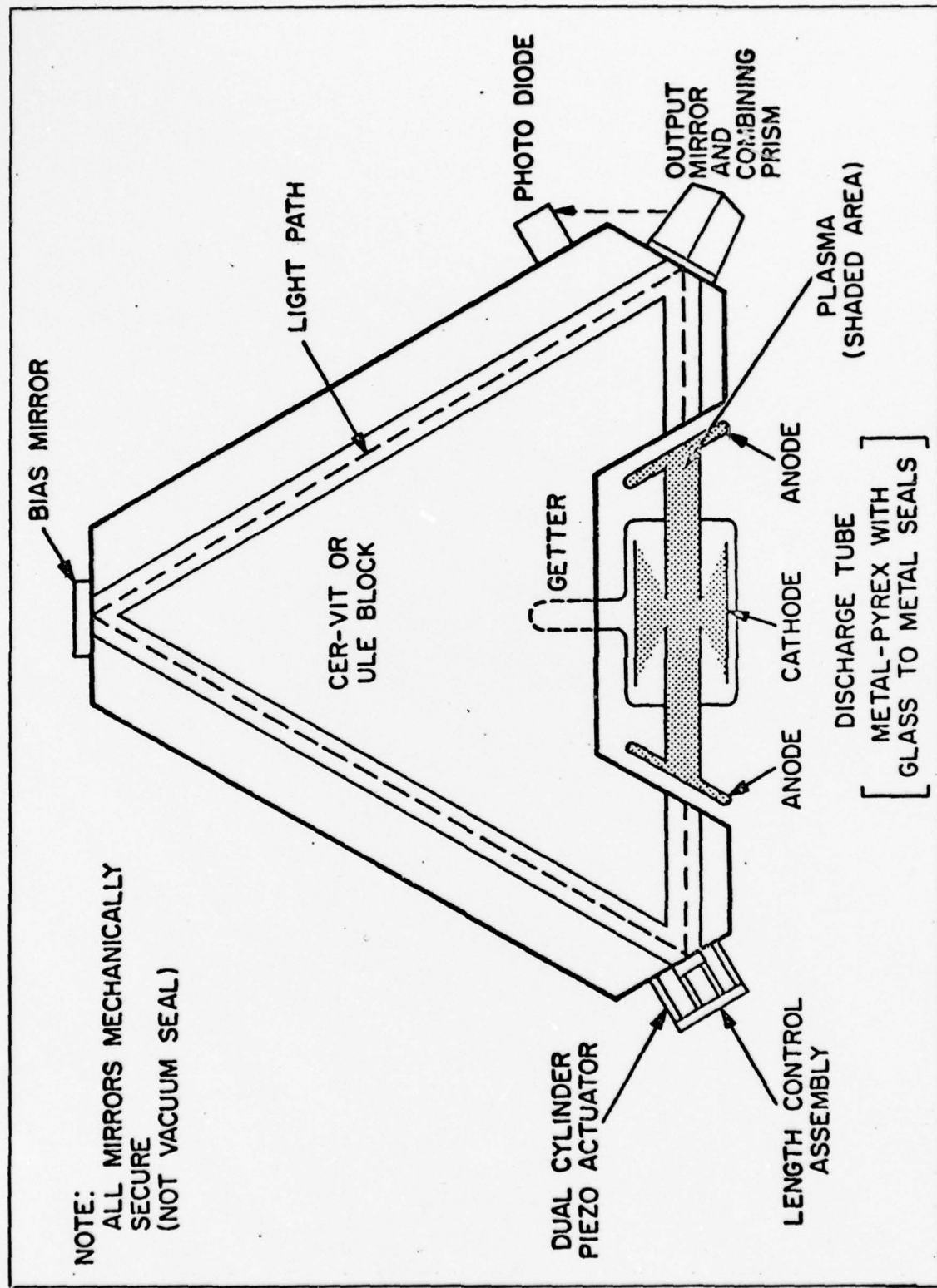


Figure II-2. Laser Gyro Optical Schematic(Ref 1)

the plane of the triangle. Mounted in one leg of the triangle is a glass-metal plasma tube filled with a low pressure mixture of helium and neon gas. At each end of the tube is a glass window to permit the light to pass through the tube (and therefore through the gas mixture). The gas is excited by passing an electrical current through it. This excites the neon atoms and results in the establishment of a clockwise and a counterclockwise beam within the optical cavity. The neon resonance frequency employed has a wavelength of 1.15 microns and is in the infrared region.

When the optical cavity is not rotating, the clockwise and counterclockwise waves have the same frequency. When the cavity is rotating, one optical path length is increased and the other is decreased. The conditions for lasing require that the total path length around the cavity be an integral number of wavelengths, and therefore the particular wavelength selected by the cavity for the clockwise beam is slightly different from the wavelength selected for the counterclockwise beam. The constancy of the velocity of light requires that the optical frequencies change also, and the resulting difference between the clockwise and counterclockwise optical frequencies are proportional to input angular rate. The count resulting from summing this frequency is therefore proportional to the total angle through which the gyro has been rotated. The relationship between input angle and output count depends upon the size and shape of the optical path and the wavelength of the optical beam, as shown:

$$\Delta f = 4AW_{ip}/\lambda L \quad (II-1)$$

$$N = \int \Delta f dt = \int (4AW_{ip}/\lambda L) dt \quad (II-2)$$

$$N = 4A \theta_{ip}/\lambda L \quad (II-3)$$

where

Δf - Optical Frequency Difference

λ - Wavelength of Light

L - Length of the Optical Cavity

A - Area of the Optical Cavity

W_{ip} - Input Angular Rate

θ_{ip} - Input Angle

N - Output Count

The mirrors defining the optical cavity each have additional functions which are:

1. The output mirror is used to extract optical information from the gyro.

2. The perimeter control mirror is adjustable to servo the cavity perimeter, to make it an integral number of the particular wavelengths for which the neon lasing medium has maximum gain. This insures maximum output and eliminates a medium dependent source of error.

3. The bias mirror is used to introduce an apparent rotation in the gyro to bias the clockwise and counterclockwise frequencies away from each other. This avoids energy-coupling

between the waves (which tends to make the waves lock to the same optical frequency) that would result in a laser gyro lower rate threshold.

The three accelerometers are identical as shown in the exploded view of Figure II-3. Each is a complete, self-contained, miniature servo-mechanism in which the torque arising from linear acceleration on a pendulous seismic element is precisely opposed by an equal capturing torque. This torque is accurately proportional to the level of DC current generated by the servo in an electromagnetic torquer. By automatically maintaining the pendulum in this condition of "force-balance" the servo accelerometer provides a high level voltage output signal, which is an accurate and continuous measure of the sustained and dynamic specific force to which it is subjected. The IMU electronics assembly contains circuitry to convert the analog signal to precise digital increments.

Electronic Assembly (Ref 1:22-24)

The IMU electronics assembly is functionally divided into three major areas as shown in Figure II-1 are:

1. Signal Conditioner
2. Laser Gyro Control
3. Power Supply

The signal conditioner operates on laser gyro and accelerometer output signals to condition the signals for multiplexing into the digital computer. The laser gyro signal conditioning consists of bias and scale factor compensations to

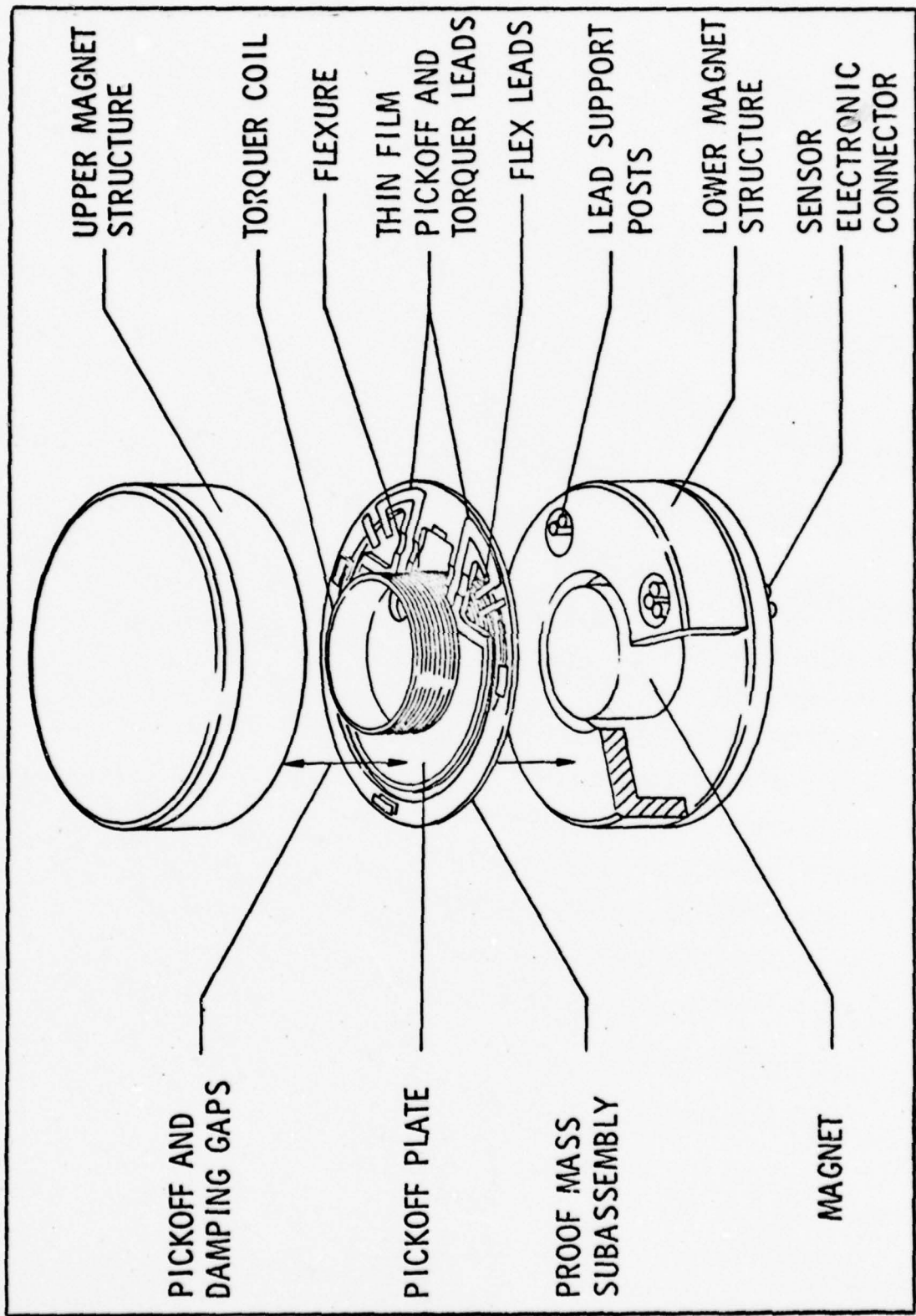


Figure II-3. Accelerometer Exploded View(Ref 6)

translate gyro output signals into scaled body angle increments. The accelerometer conditioning consists of a pulse converter to digitize the accelerometer analog outputs. The accelerometer outputs are digital representations of body axis incremental velocities since the pulse rate is proportional to specific force.

The signal conditioner also contains a customized interface to accomodate gyro and accelerometer data transfer into the system's general-purpose computer. Upon address by the computer, the gyro and accelerometer angle and velocity increments are multiplexed in 12-bit parallel form into the computer.

The laser gyro control contains the circuitry necessary for satisfactory operation of the three laser gyros. Each laser gyro requires the following three closed loop control servos: optical bias current regulation, cavity path length control, and gas discharge tube current regulation.

The power supply contains regulated dc-to-dc converters for all of the primary IMU power requirements. This system operates off a 28 volt D.C. external power supply fused at 6 amperes.

III. Laboratory Test Set-Up

System Description

The system block diagram of the laboratory test set-up to obtain and process digital data from the IMU is shown in Figure III-1. The sensor assembly fixture, data monitor controller, multiplexer, and programmer were designed to interface with the Genisco rate table, IMU electronic assembly digital computer interface, and Cipher magnetic tape recorder. Then with the IMU in desired positions, data is recorded on magnetic tape and processed by the FORTRAN program on the CDC 6600 digital computer.

Utilizing the electronics assembly computer-compatible interface module that converts the sensor information to velocity and angular rotation increments, operation of the IMU was controlled in the absence of a computer by the data monitor controller. It permits each of the gyro and accelerometer output registers to be sampled for intervals selected by the pulse generator, and present the registers contents in octal form on an output display. These six data words strobed by the data monitor controller are multiplexed from the IMU via parallel data lines, with a data format in two's complement negative numbers, 11 bit plus sign.

The multiplexer, after receiving the register contents, buffers the data words and processes the twelve bit words into 6 parallel data lines required by the magnetic tape recorder. The multiplexer also attaches an octal code word (4444) to each data group which will be used by the CDC 6600 digital computer to

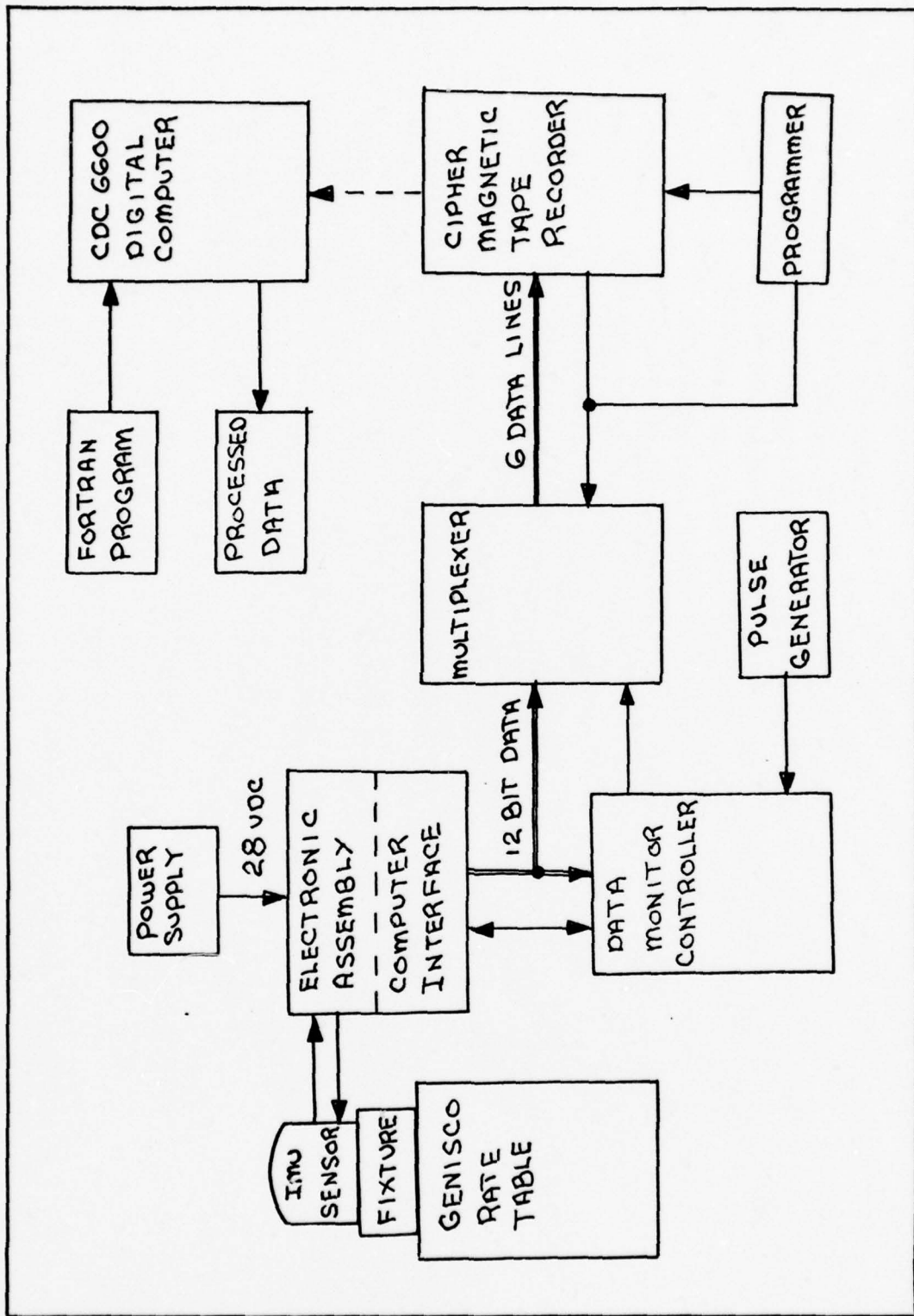


Figure III-1. Block Diagram of the Laboratory Test Set-Up

identify a data group.

The magnetic tape recorder operating in the continuous mode (800 bytes/in) records the data at a rate of 200,000 characters/sec. To meet requirements imposed by the CDC 6600 read capabilities, the programmer applies an inter-record gap every 10 seconds or 200,000 characters.

The recorded magnetic data tape is processed on the CDC 6600 digital computer by a FORTRAN search routine for the octal code (4444) attached to each data group strobed by the data monitor controller. Each group is then sorted into gyro and accelerometer data to be printed or further processed according to specific test requirements.

Equipment Description

IMU/Digital Computer Interface (Ref 1:30-32). The digital computer interface was designed by Sperry to accomodate IMU interfacing with a digital computer. Upon command the gyro and accelerometer angle and velocity increments are multiplexed in 12-bit parallel form with identities for each of the six data words generated. The interface block diagram is shown in Figure III-2.

In operation the pulse output of both the laser gyros and accelerometers are summed in six individual up/down accumulators whose sums represent body angle and velocity increments. The gyro accumulators have 11 bit plus sign summing capability. The gyro angle increments are scaled to approximately 13.3 arc seconds which is 7.56 degrees for full accumulation. Then with

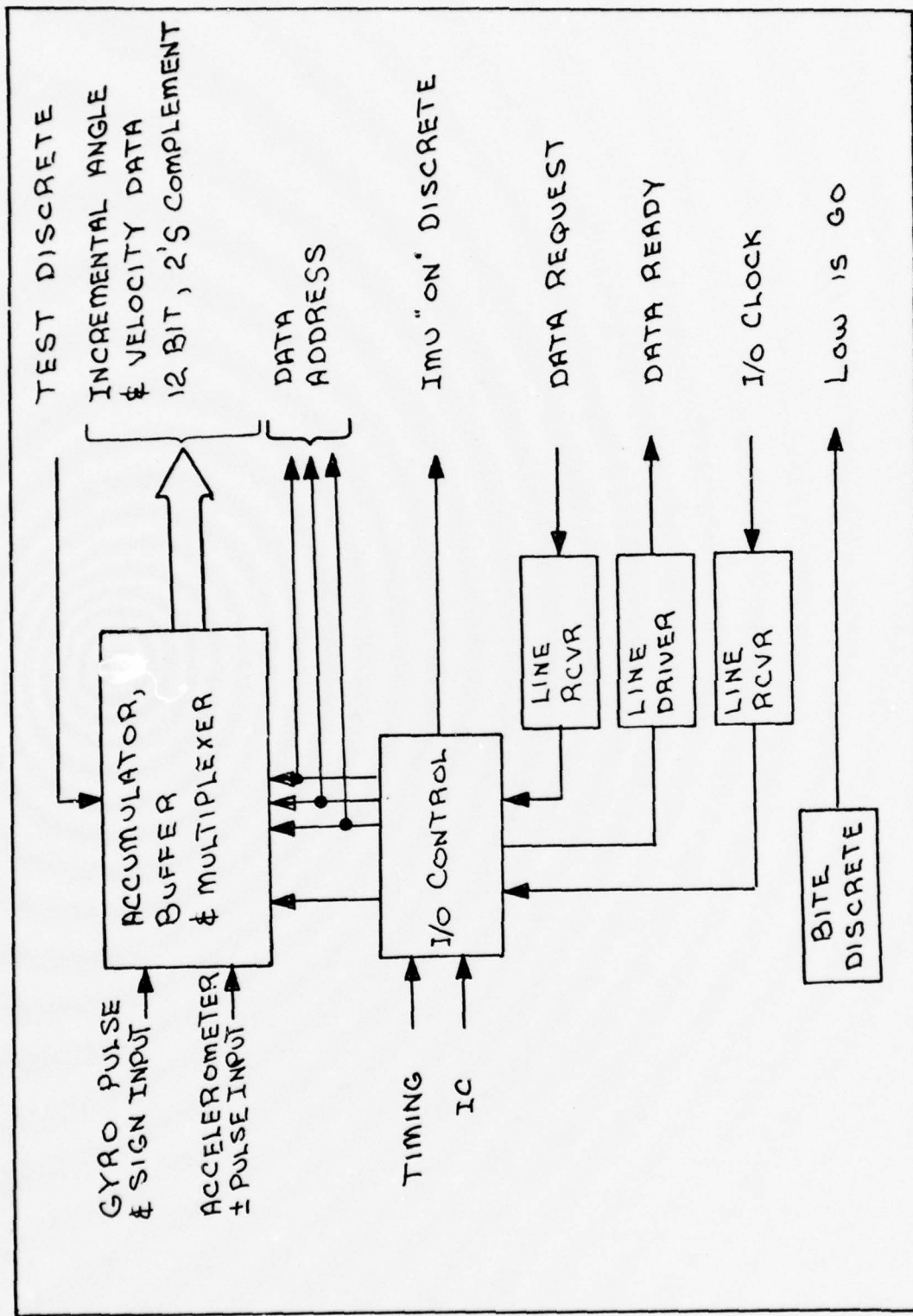


Figure III-2. IMU/Computer Interface Block Diagram

the output data rate of 100 readouts per second, which is a 100 Hz sampling rate from the data monitor controller, provides 756 degrees per second accumulator rate handling capability.

The accelerometers have six bit plus sign summing capability. Accelerometer plus scaling is approximately 0.0420 feet per second which is 2.65 feet per second for full accumulator. Again, the output data rate of 100 per second provides a 265 foot per second squared acceleration handling capability which is greater than 8 g.

These accumulators operate continuously to gather all the gyro and accelerometer output data. On receipt of a data request discrete from the data monitor controller, each of the six accumulators have their contents transferred onto storage registers and are cleared ready to continue counting without loss of data.

When the transfer to the holding registers is completed the interface module generates a data ready discrete that is used by the data monitor controller to indicate the data transfer into the multiplexer and output display. Also the data address lines are set to identify the on-line data as gyro "A" output. Data monitor controller clock pulses are then received at 5 micro-second intervals that multiplex the contents of the six data registers with their appropriate data identification as shown in Figure III-3. This data transfer sequence is repeated every 0.01 seconds when the data request rate is 100 Hz.

In addition to data interface described above, the interface includes three other IMU condition descretes:

1. IMU "ON" discrete, has a high state when the IMU is

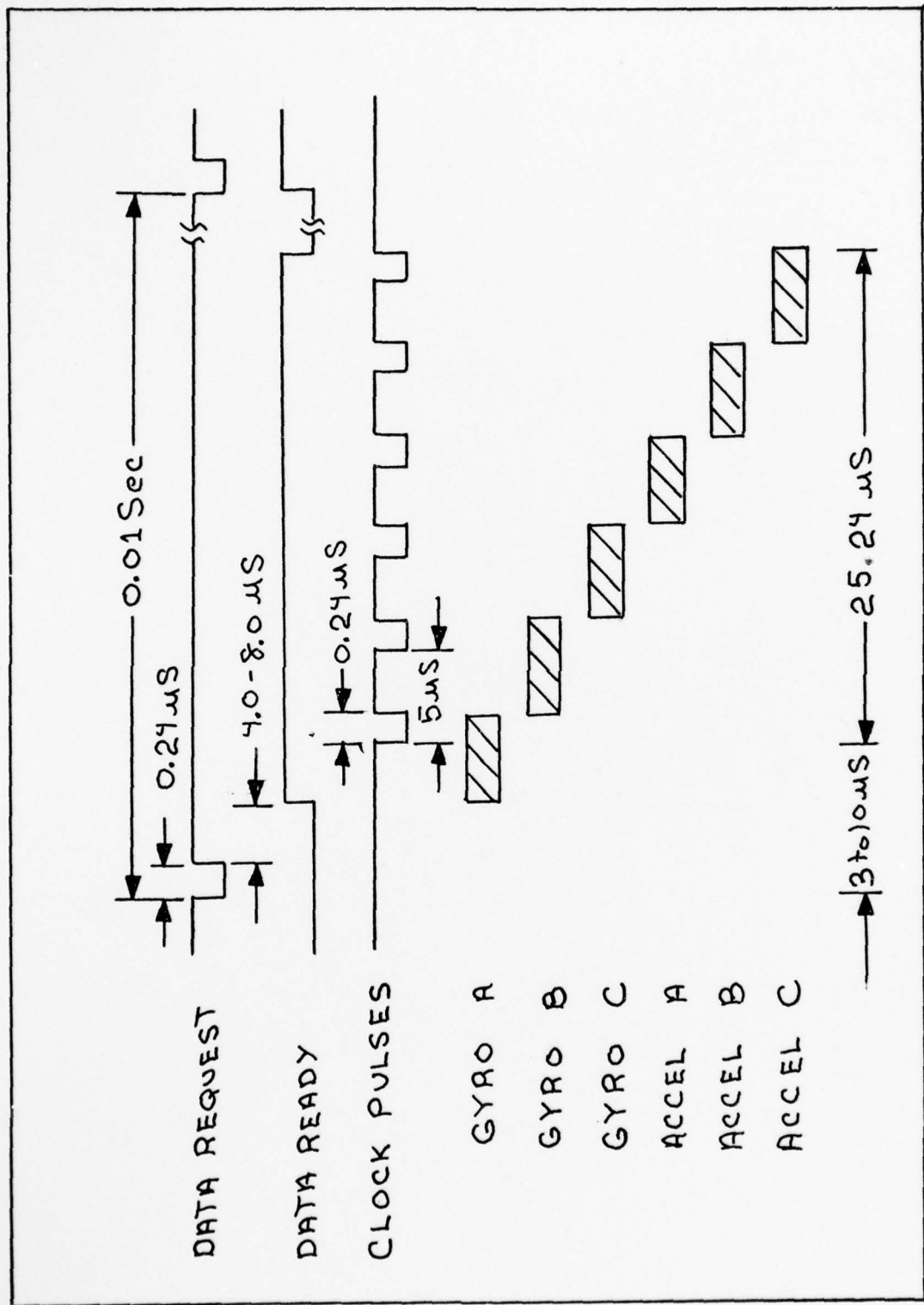


Figure III-3. IMU/Computer Timing Diagram

operationally ready.

2. BITE discrete, has an output that stays low when all of the IMU BITE (Built-In-Test-Equipment) monitored signals are satisfactory.

3. TEST discrete, on receipt of a low signal (steady level) the six data accumulators are preset to fixed data increments.

Data Monitor Controller. The data monitor controller, which is a modified Sperry design, was built to obtain digital data from the IMU via the IMU/Computer interface in the absence of a computer. This equipment permits each of the three gyro registers and each of the three accelerometer registers to be sampled for intervals selected on the pulse generator. The six data words are transferred to the multiplexer for processing and any desired register content is presented in octal form on an output display. Also IMU operating discretes are monitored and the test discrete controlled. The block diagram for the data monitor controller is shown in Figure III-4.

In operation the pulse generator is set to the desired rate in which the IMU is to be sampled. The minimum rate is a function of the accumulators handling capability of the IMU/Computer interface and the maximum rate (800 Hz) is due the multiplexer. Throughout this thesis 100 Hertz has been selected as the desired rate. This generates the data request discrete every 0.01 seconds and when received by the IMU/computer interface a data ready discrete is generated. Upon receiving data ready the

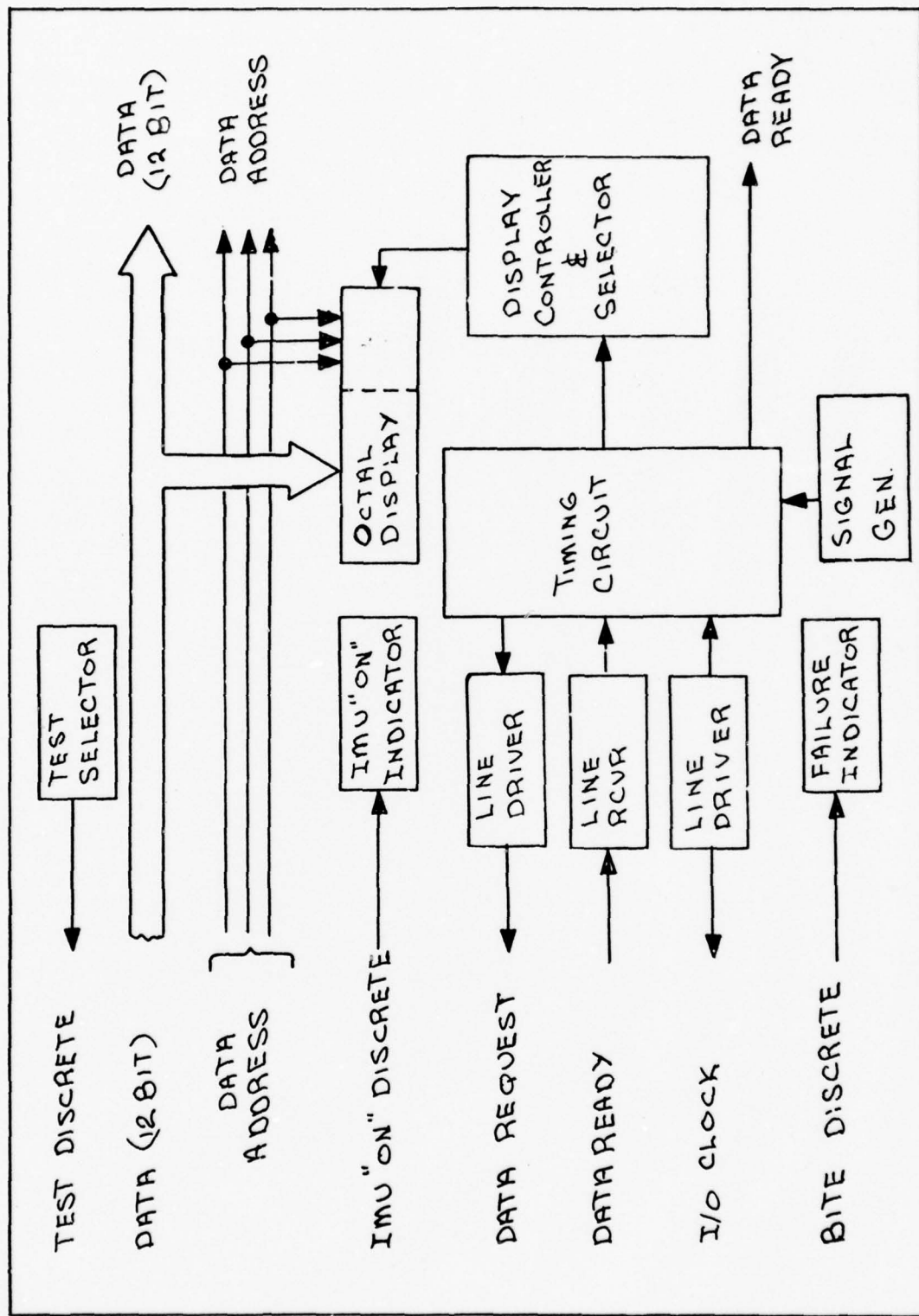


Figure III-4. Data Monitor Controller Block Diagram

data monitor controller initiates clock pulses to multiplex data from the holding registers. When the contents of the six data registers are removed, the data ready discrete is removed until the next data request is received as shown in Figure III-3. The reason the data words are strobed within 30 microseconds of the 0.01 second sample rate is to obtain data from all six instruments at essentially the same time. The assumption then is that the data taken within a 30 microsecond period is instantaneous.

The data word desired to be displayed in octal form on the output display is selected by processing the clock pulses through an up/down counter and controlling the display rate. The data address is also displayed to indicate that the correct data word has been selected.

The test mode enable discrete is selected on the data monitor controller which permits fixed test words wired into each register of the IMU/Computer interface to be displayed. The chart on Table III-I shows the values of the test words for the octal displays according to data address. Also the binary form is shown, which was used extensively in designing the multiplexer and CDC 6600 FORTRAN Program. Figure III-5 presents the signals in the test mode to show the relationship between data request, data ready, clock pulses, data address and data words. The IMU "ON" and BITE discretes are monitored by light indicators and a schematic diagram of the data monitor controller is shown in Figure A-1 and A-2 of Appendix A.

Multiplexer. The multiplexer, a completely new design,

Table III-I. Test Words Chart

ADDRESS	DECIMAL VALUE	BINARY VALUE								OCTAL VALUE		
		11	10	9	8	7	6	5	4	3	2	1
0	211	0	0	0	0	0	0	0	0	0	0	323
-	1418	0	0	-	0	0	0	0	0	0	0	2612
2	535	0	0	-	0	0	0	0	0	0	0	1027
3	32	0	0	-	0	0	0	0	0	0	0	40
4	30	0	0	-	0	0	0	0	0	0	0	36
5	21	0	0	-	0	0	0	0	0	0	0	25
DATA MONITOR CONTROLLER DISPLAY												
0	0	3	6	9	6	9	6	9	6	9	6	3
-	2	2	1	0	2	1	0	2	1	0	2	2
2	2	2	1	0	2	1	0	2	1	0	2	7
4	3	3	2	1	0	2	1	0	2	1	0	0
5	5	5	4	3	2	1	0	2	1	0	2	0
7	7	7	6	5	4	3	2	1	0	0	0	0
5	5	5	4	3	2	1	0	2	1	0	2	0

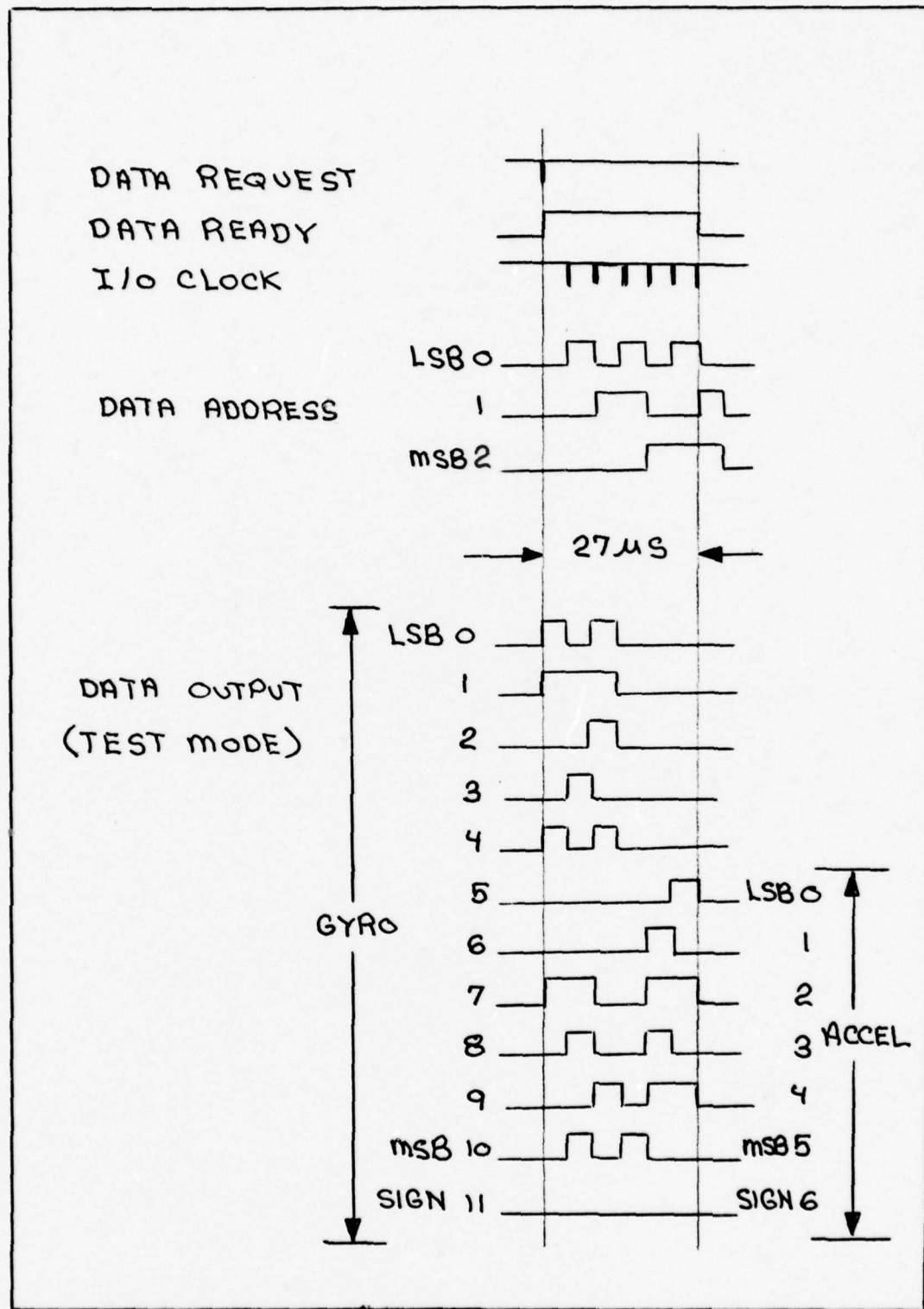


Figure III-5. Data Monitor Controller Signals

was built to buffer and multiplex the six, 12 bit, data words to interface with the 7 track Cipher magnetic tape recorder. It consists of four major elements:

1. Decoder
2. Buffers
3. Multiplexers
4. Binary Counter

The functional relationship of these elements are shown in the system block diagram in Figure III-6.

The decoder operation within the 0.01 second sampling period receives the 3 bit binary data addresses and produces six clock pulses as shown in Figure III-7. Using the clock pulses as identifiers, the six data words are transferred into 12 buffers (6 bits per buffer) and maintained until cleared by

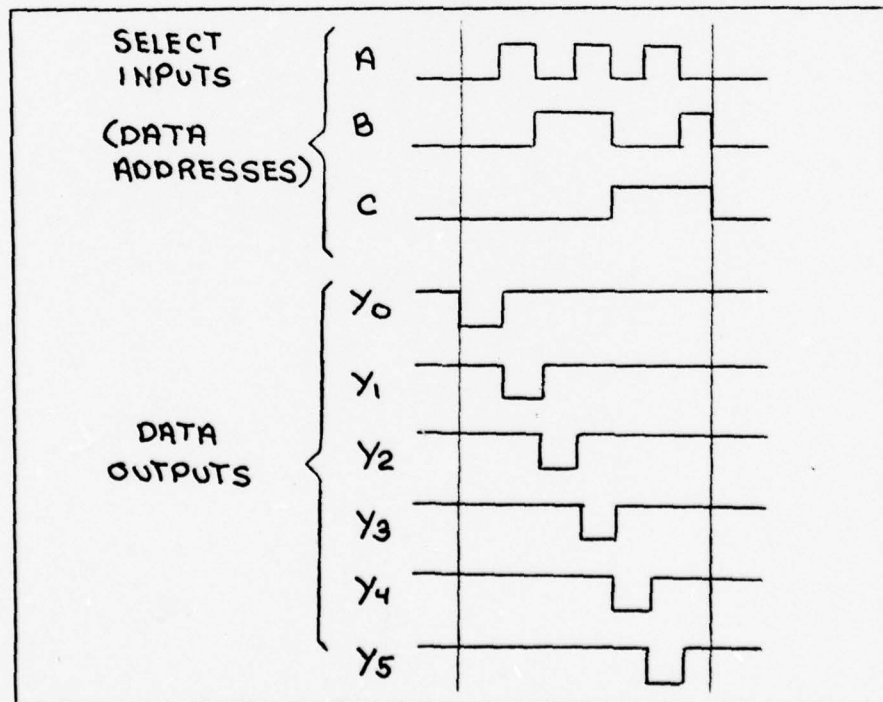


Figure III-7. Decoder Signals

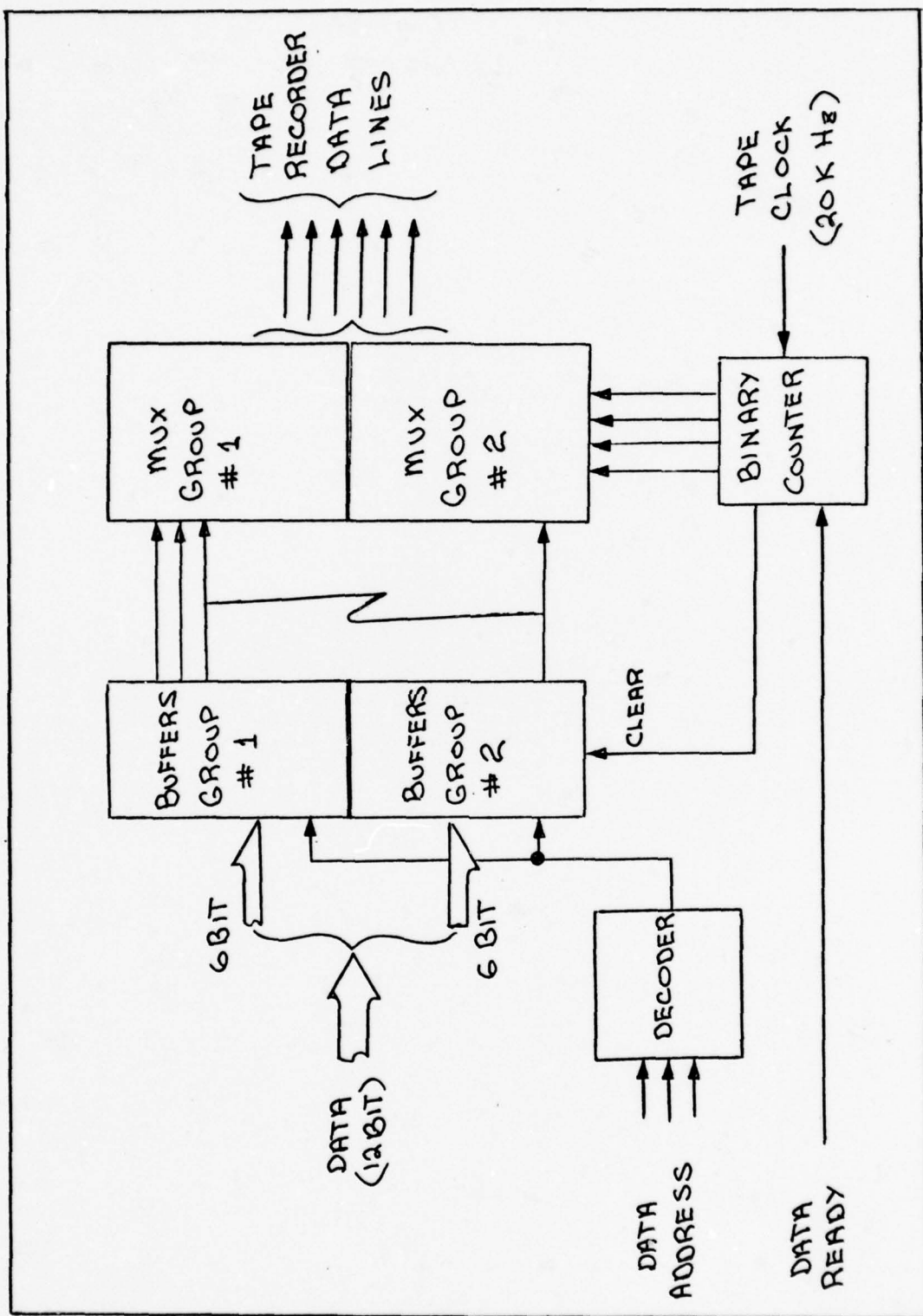


Figure III-6. Multiplexer Block Diagram

the binary counter. Upon removal of the data ready discrete, which signals that all data is transferred to the buffers, the binary counter is activated.

The counter using the 20K Hertz clock from the magnetic tape recorder strobos(4 bit binary) the 6 multiplexers which are hard wired in logical sequence to the buffers. When all the data is multiplexed into the tape recorder via 6 parallel data lines, the buffers are cleared.

Since each multiplexer contains 16 inputs and only 12 were required, a code was wired into each multiplexer. This octal code word(4444) was attached to the end of each data group of six data words. Figure III-8 shows the signal relationship of the data ready, tape clock, binary counter and multiplexed data words with the test mode selected by the data monitor controller. Also a schematic diagram of the multiplexer is shown in Figure A-3 thur A-9 of Appendix A.

As shown the multiplexer required approximately 600 micro-seconds to multiplex the data after being transferred within 27 micro-seconds from the IMU. In total 630 micro-seconds maximum is required to process data from the IMU within the 0.01 second sampling period. Therefore, the maximum sampling period determined without data overlapping is approximately 800 Hertz.

Programmer. The programmer, a completely new design, was built to control the functions of the Cipher(model 85H) magnetic tape recorder when operating in the continuous recording mode. Its requirements were due to read(Buffer-In) capabilities of the

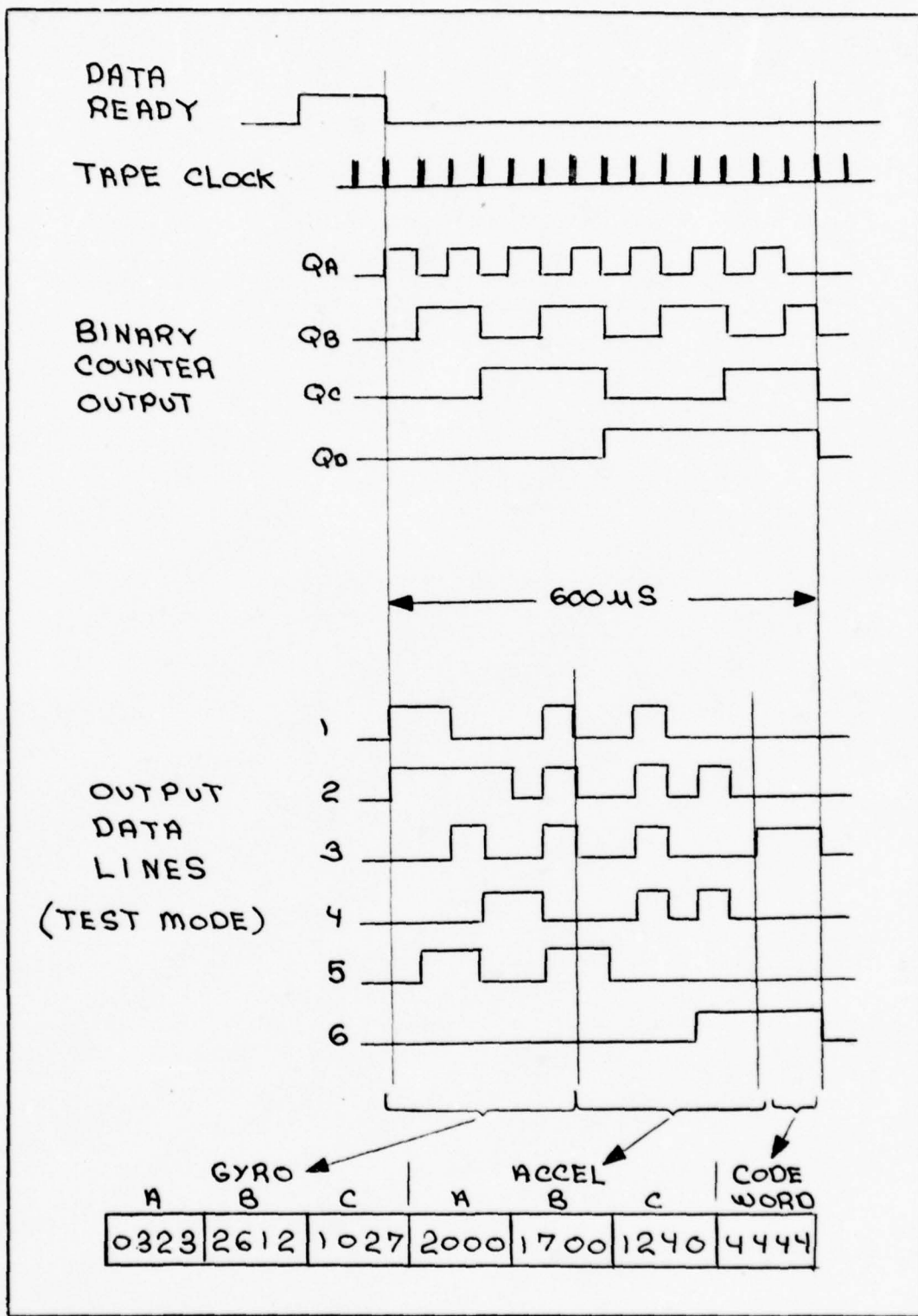


Figure III-8. Multiplexer Signals

CDC 6600, which processes the recorded data tapes, and the recording mode selected to handle the data rates from the multiplexer. Figure III-9 is a block diagram of the functional relationship of the programmer to the Tape recorder.

The Cipher, Model 85H, high performance computer-compatible Magnetic tape recorder is a seven-track system; six (6) of the tracks are data channels while the seventh is the parity channel. The continuous recording mode was selected, since the minimum time to generate an inter-record gap was required, to reduce data loss when the IMU is sampled at high rates.

In the continuous mode the run command is given which accelerates the tape. When operating speed is reached (25 in/sec), the busy indication is removed and the 20KHz write clock is enabled. Data is then clocked onto the tape at 20,000 characters per second (i.e. 25 in/sec x 800 bytes/in). When the desired record length of 200,000 characters (10 sec) is reached, an interrecord gap is generated without stopping the tape. This is accomplished by adding up 200,000 clock pulses and generating a pulse to make the Insert Check Characters (ICC) input true. This input produces a busy indication and inhibits the write clock. After the inter-record gap has been generated the busy output is removed and the clock output returned. Since the busy signal is 0.03 seconds there was a loss of three data groups, which is related to the sampling rate (0.01 sec) of the data monitor controller.

The next record is then started and the sequence is repeated for as many records desired. When the desired amount is recorded

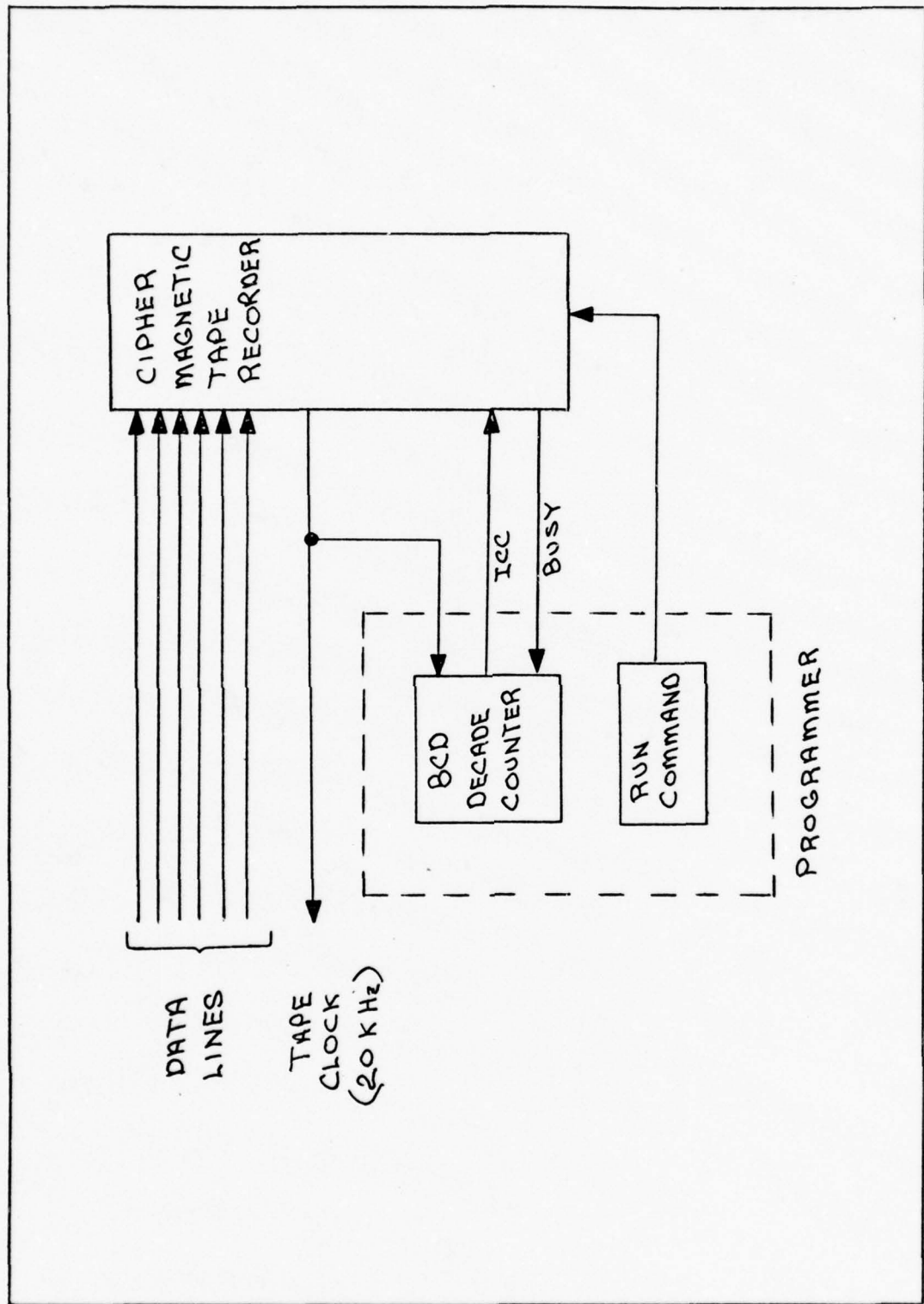


Figure III-9. Programmer Block Diagram

the run command is removed to stop the tape. If a file gap is desired after a number of records, it must be initiated by the manual controls on the tape recorder. Also a file gap must be initiated to enable the rewind sequence. The signal relationships are shown in Figure III-10 and a schematic diagram of the programmer is in Figure A-7 of Appendix A.

Test Fixture. The test fixture was designed and built to allow the IMU sensor assembly to be oriented in any desired position while attached to the Genisco rate-table. It is a two gimbaled aluminum structure that maintains the IMU center of gravity aligned with the rate-tables axis. The fixture is shown in Figure III-11 with the sensor assembly.

The outer gimbal was bolted to the center of the rate-table which can be rotated about the local vertical at any desired rate. The inner gimbal can be positioned at any angle within the outer gimbal and the sensor assembly can be rotated within the inner gimbal. Therefore, the sensor assembly sensitive axes can be positioned in any desired orientation for static testing and rotated for dynamic testing.

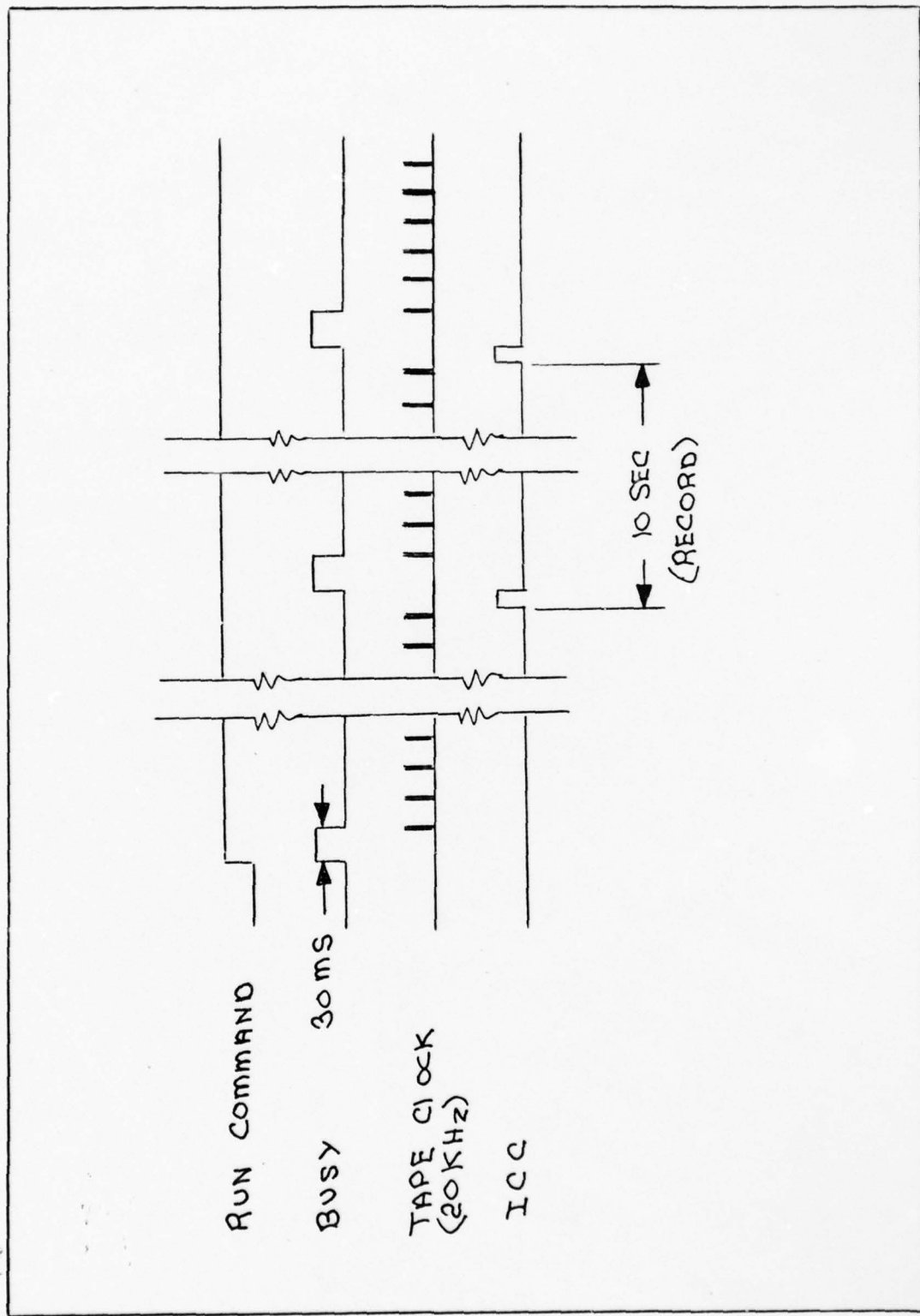


Figure III-10. Programmer Signals

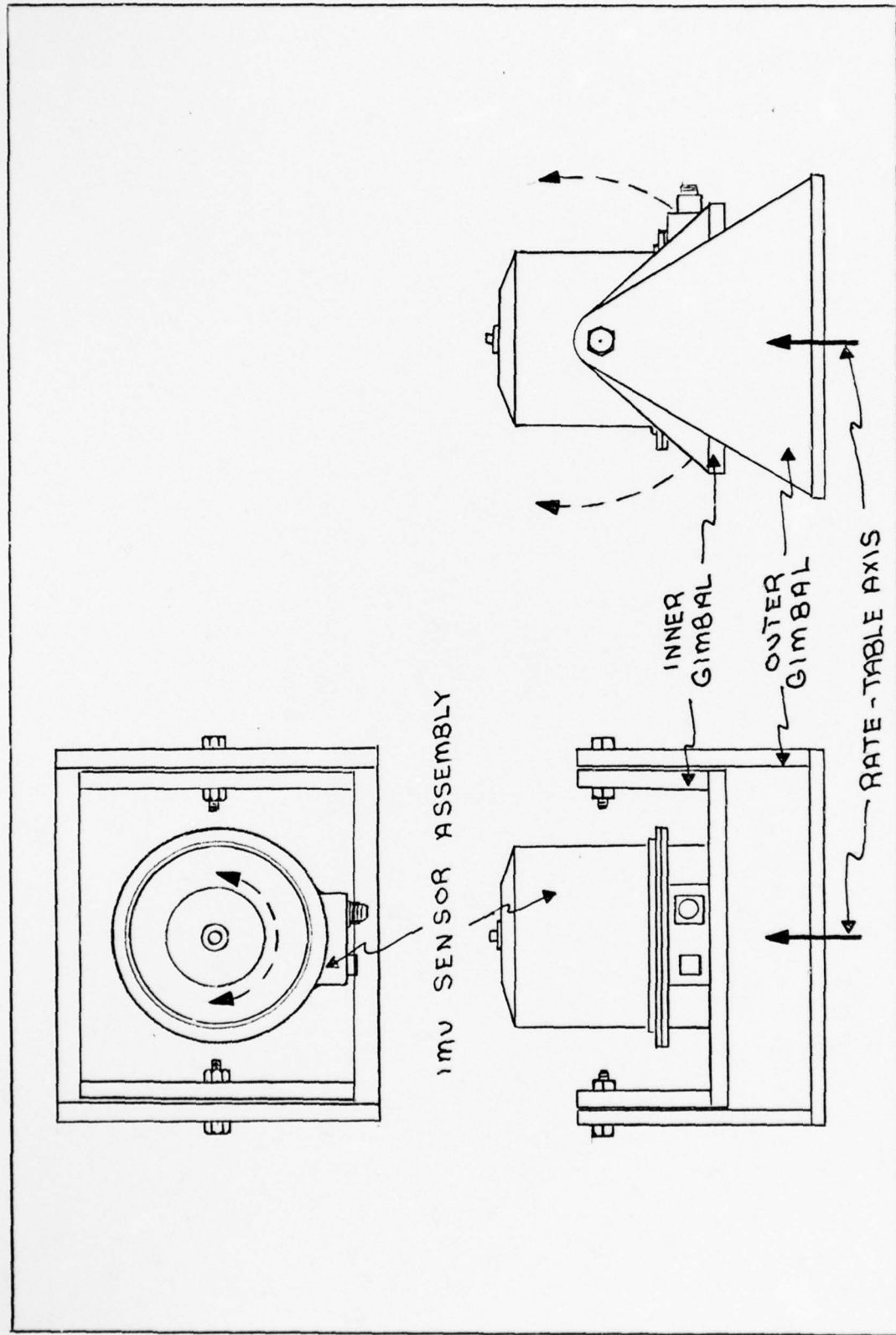


Figure III-11. Sensor Assembly Test Fixture

IV. Test Data Processing

Computer Program Description

The following FORTRAN Program was developed to process the data recorded on the magnetic tapes by the CDC 6600 digital computer. The major steps in the computer program are:

1. Read in the control data to determine the number of records and files to be processed and units of the output data.
2. Buffer in the data records (20,000 octal words per record) from the magnetic tape and determine the record and file number.
3. Process the data records, using a search routine for the code attached to each data group and summing the data to obtain the desired output information.
4. Write out the results, along with enough of the information to identify the record, file, and data units.

The flow chart for the major steps listed above is shown in Figure IV-1 which illustrates that each record on tape is read, processed, and written in sequence until all specified control data is completed.

The control data which specifies the number of records, files, and units of the data to be processed is accomplished with a data statement. Since the number of files and the records per file is determined when the tape is recorded, then all data records to the specific file and record specified on the data statement will be processed. The units of the data have a direct

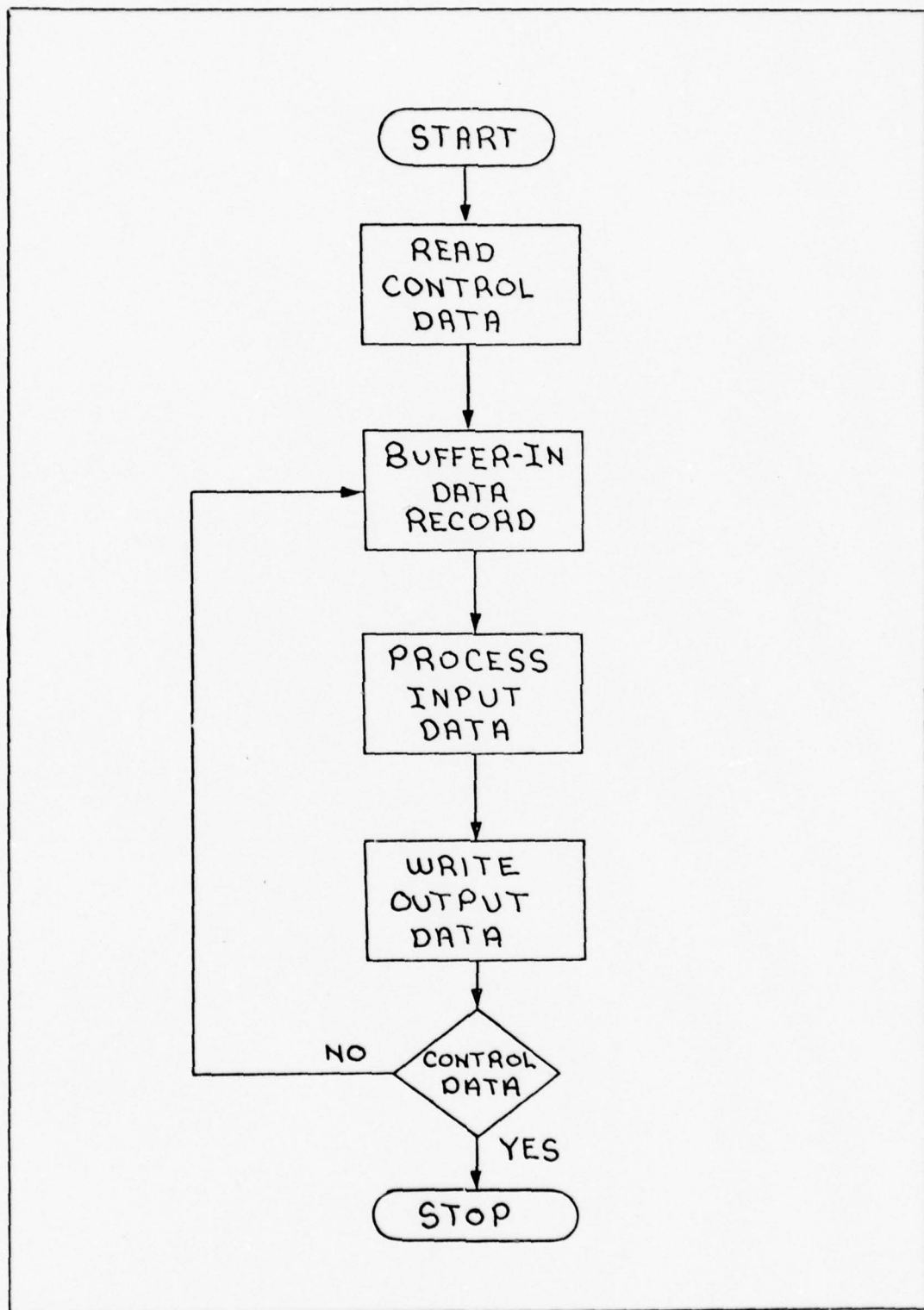


Figure IV-1. Program Major Steps Flowchart

relationship to sampling rate of the IMU selected by the data monitor controller. For example, if the sampling rate were 100 Hz then there would be 1000 groups of data words per record. Then if every 100 groups of data were summed after being processed, the units would be pulses per second, and 10 groups of data in pulses per second will be listed per record.

The Buffer-In statement causes one record of data (20,000, 60 Bit, Octal words) to be transmitted from the magnetic tape to a storage location. Also designed is the fact the magnetic tape is 7-track and recorded in binary (odd parity). The unit function checks the buffer in operation for an end-of-file to indicate different files that were recorded. The length of the record is ascertained through the length function which determines the number of 60-bit words read.

The processing of a record of data involves a search routine which samples every 20,000 octal words in sequence for the octal code (4444) attached to each data group. This is accomplished by using the intrinsic functions, SHIFT and MASK, and logical expressions which essentially samples the entire 60-bit word every 6 bits and checks the 6 bits for the octal word (44). If the octal word (44) is located then the next 12 bits are checked for the code word (4444).

When the code is located the subroutine SORT is called which separates the 12 bit gyro and 7 bit accelerometer data from the data group. This data group usually is located within three 60 bit words, and a starting point is given to SORT to indicate where the group is located. When the data is sorted,

then subroutine ASSIGN is called which transforms the binary data to integer values. Since the data is in the form sign plus two's complement, all gyro data (11 bits + sign) and accelerometer data (6 bits + sign) are checked for polarity before assigning an integer value.

Then the numerical value (according to the IMU sampling rate) for each gyro and accelerometer is sorted in an array until the specific number IADD is obtained. When IADD is obtained, which means the specified number of data groups has been stored, then subroutine ADPULSE is called. ADPULSE sums the number of data groups stored and printed is the number of pulses per unit time selected in the control data for each gyro and accelerometer. A more detailed flowchart of the program is shown in Figure IV-2 and a computer listing is in Appendix B.

Typical Test Data

Typical test data recorded from the IMU is shown in Table IV-I. When the data was recorded the sampling rate of the IMU was 100 Hertz and for processing the control data IADD was set to 100 to sum every 100 data groups which produces units of pulses per unit as indicated. Since each record is 10 seconds then 1000 data groups should be recorded per record. However, the value of total sorted indicated at the end of each record is the exact number of data groups recorded in that specific record. Therefore, due to the accuracy of the pulse generator used with the data monitor controller, the number of data groups per record may vary slightly as shown in record two.

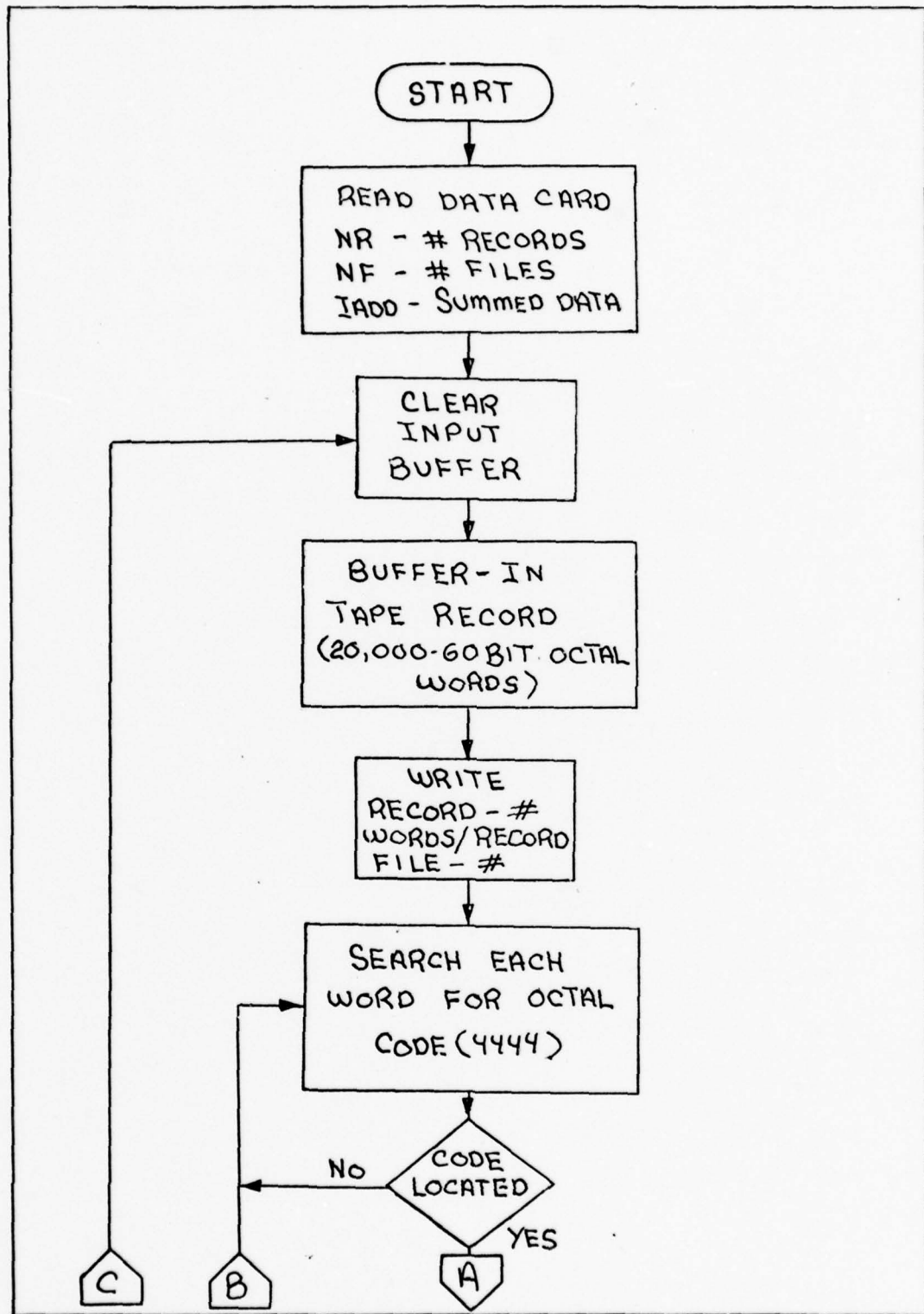


Figure IV-2. Detailed Program Flowchart

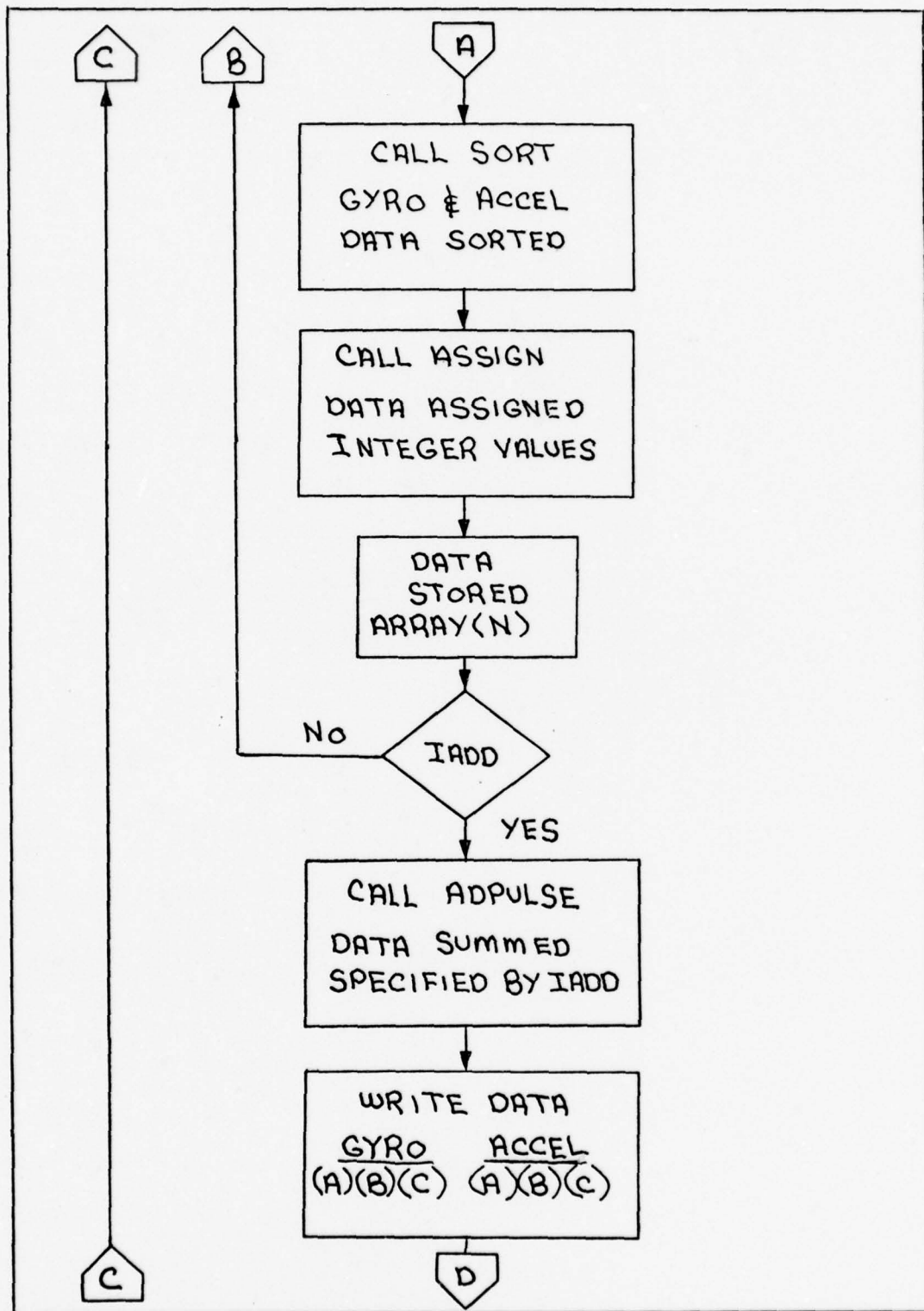


Figure IV-2. (Cont.)

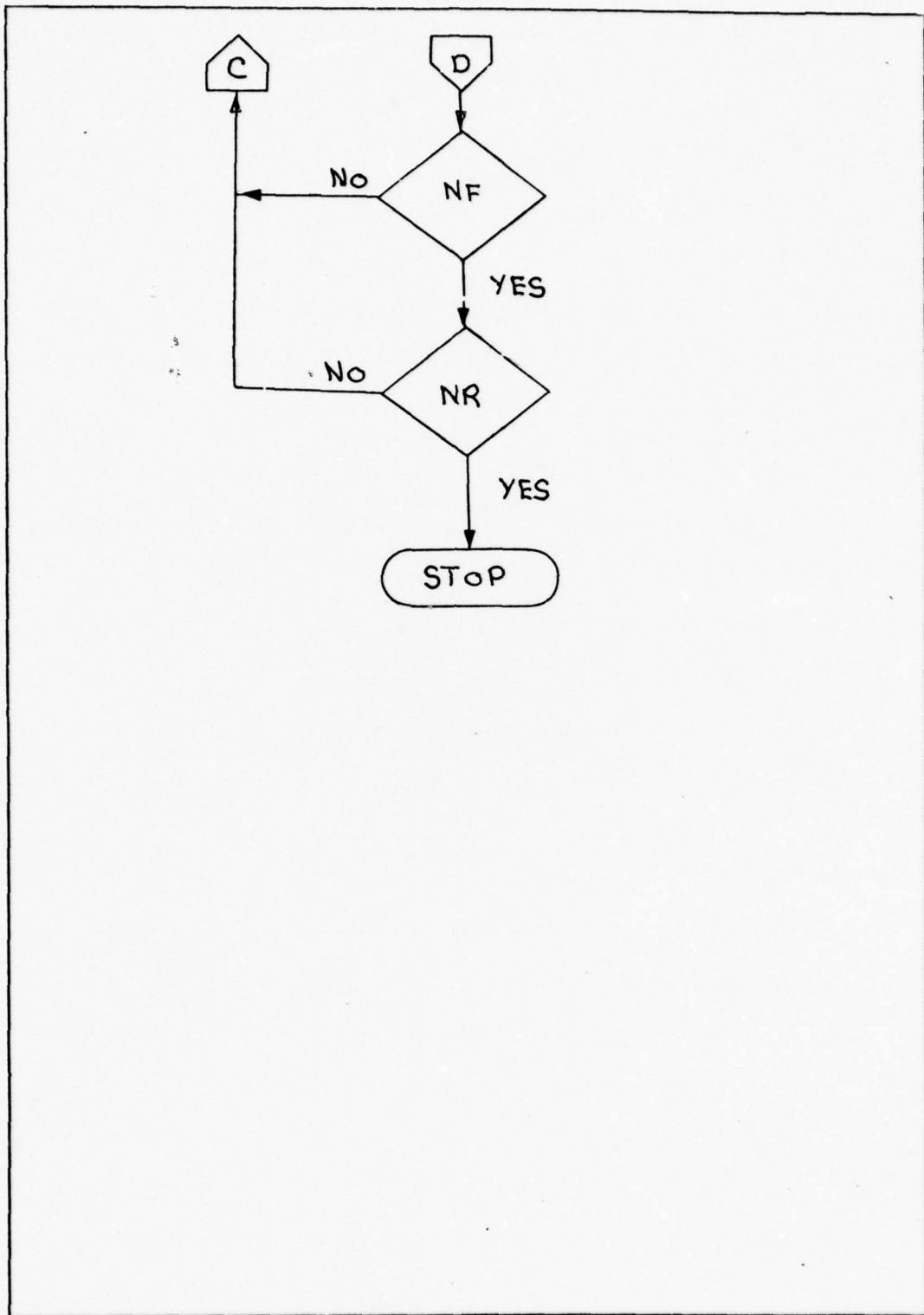


Figure IV-2. (Cont.)

Record one contains 9 seconds of data with the IMU operating in the test mode selected by the data monitor controller. The values processed for the gyros and accelerometers are equal to 100 (IADD) times the decimal values in the test word chart of Table III-I. This indicates that the laboratory set-up was functioning properly.

Record two contains 10 seconds of actual test data with the IMU orientated to allow equal components of gravity along the sensitive axes. The total sorted was 999 which allowed only 9 summed groups of data to be listed. This demonstrates the requirement for an accurate sampling rate to properly process test data. Also gyro "A" indicates a bias problem.

Table IV-I. Typical Test Data

RECORD 1 LENGTH 18001 FILE 1
UNITS (PULSES/SEC)

GYRO		
(A)	(B)	(C)
21100	141800	53500
21100	141800	53500
21100	141800	53500
21100	141800	53500
21100	141800	53500
21100	141800	53500
21100	141800	53500
21100	141800	53500
21100	141800	53500
21100	141800	53500
21100	141800	53500
21100	141800	53500
21100	141800	53500
21100	141800	53500
21100	141800	53500
TOTAL SORTED	900	

RECORD 2 LENGTH 20100 FILE 1
UNITS (PULSES/SEC)

GYRO		
(A)	(B)	(C)
-425	-4	-444
-427	-7	-444
-426	-3	-444
-427	-5	-445
-427	-6	-444
-425	1	-444
-427	-7	-444
-426	-2	-444
-428	-5	-445
TOTAL SORTED	999	

V. Calibration Test

Model Equations

The calibration sequence was developed to determine the bias and scale factors for the gyros and accelerometers by positioning the IMU with respect to a master reference. The model equation selected (since only bias and scale factor were of interest) was first order which expresses instrument output in terms of bias, scale factor, and the reference input. The accelerometer model equation is:

$$A = K_0 + K_1 \dot{F}_i \quad (V-1)$$

$$\dot{F}_i = a_i - g_i \quad (V-2)$$

where

A - Accelerometer Output (pulses/sec)

K_0 - Bias (pulses/sec)

K_1 - Scale Factor (pulses/ft/sec)

\dot{F}_i - Specific Force Along Input Axis (ft/sec/sec)

a_i - Acceleration Along Input Axis (ft/sec/sec)

g_i - Gravity Component Along Input Axis (ft/sec/sec)

The gyro model equation is:

$$\dot{\omega} = K_0 + K_1 \omega_i \quad (V-3)$$

where

$\dot{\omega}$ - Gyro Output (pulses/sec)

K_0 - Bias (pulses/sec)

K_1 - Scale Factor (pulses/sec)

ω - Rotation Rate Along Input Axis (sec/sec)

Assuming the sensor axes are orthogonal within the IMU sensor assembly as shown by Sperry in Figure V-1. The accelerometers require a static 6-position test and the gyros a dynamic 6-position test to determine the model equations coefficients. These tests will allow the three gyros or accelerometers to be calibrated simultaneously in one complete sequence.

Static 6-Position Test

Test Description. The static 6-position test was conducted to determine the accelerometers bias and scale factors by positioning the IMU with respect to the earth's gravitational field. The earth's gravity vector was positioned with respect to the three orthogonal accelerometers as shown in Figure V-2. The angles θ and ϕ were used to define the components of gravity

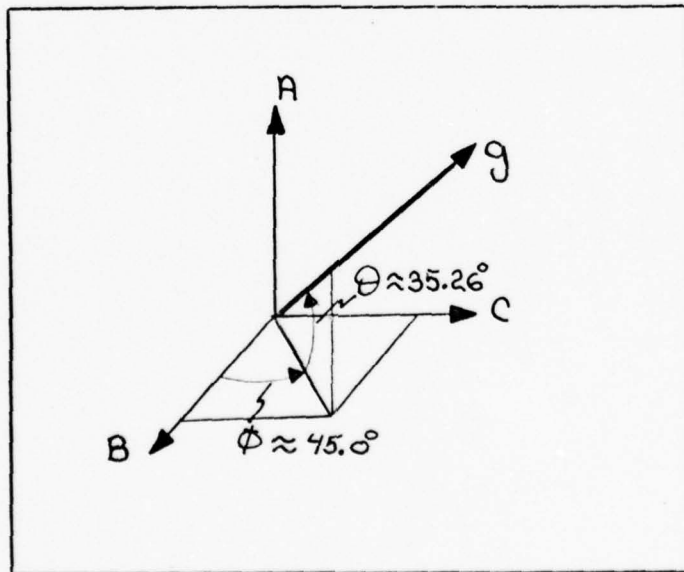


Figure V-2. Accelerometers Reference Position

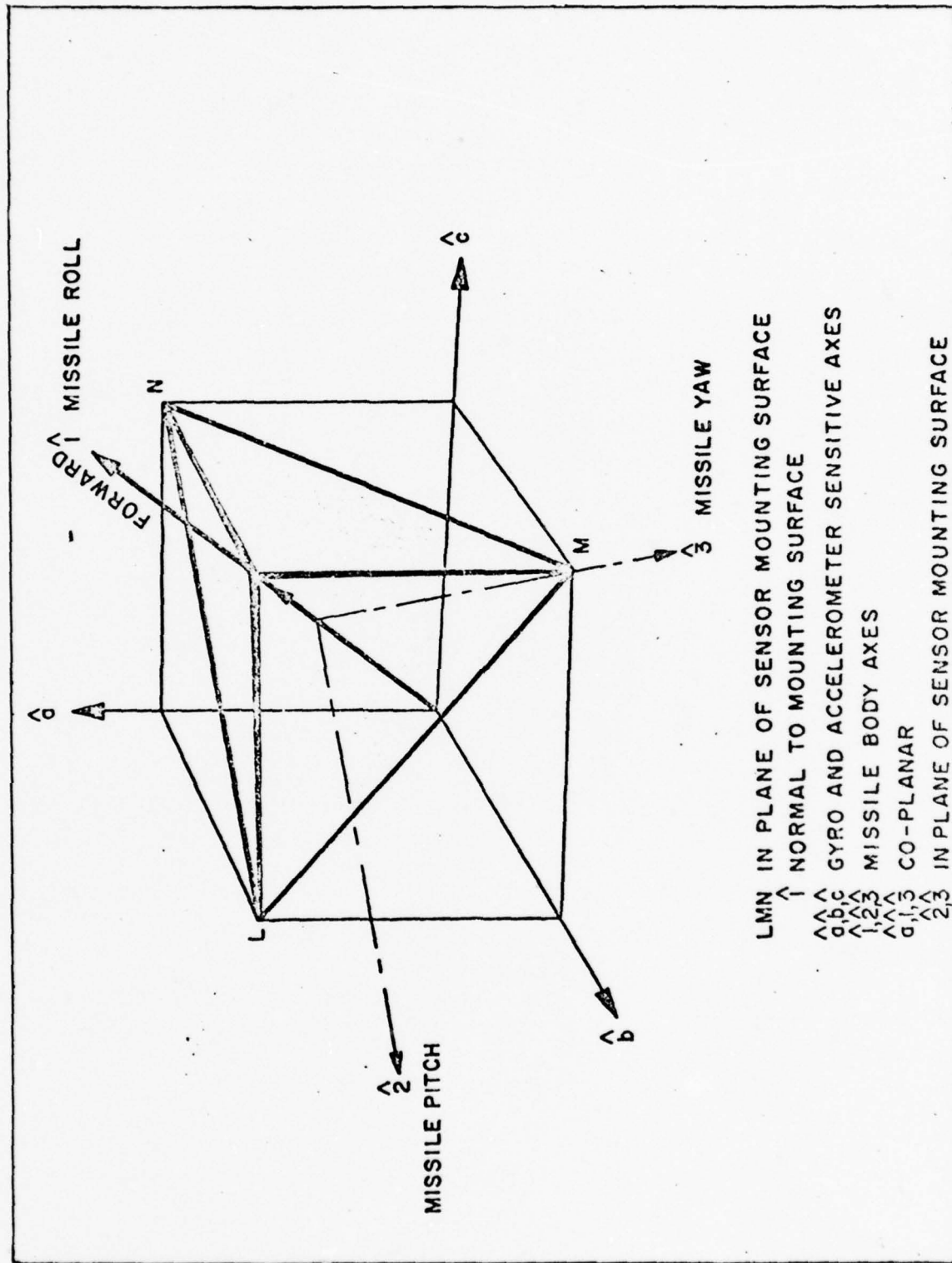


Figure V-1. IMU Sensitive Axes Orientation(Ref 1)

along the input axis for each accelerometer. Since the angles θ and ϕ are unknown the following non-linear equations were developed from model equation (V-1):

$$A_a = K_{0a} + K_{1a} g \sin \theta \quad (V-4)$$

$$A_b = K_{0b} + K_{1b} g \cos \theta \cos \phi \quad (V-5)$$

$$A_c = K_{0c} + K_{1c} g \cos \theta \sin \phi \quad (V-6)$$

With 3 equations and 8 unknowns it was required to position the IMU in the 6 positions shown in Figure V-3. This generates 18 equations with 18 unknowns as shown in Table V-I. Since the number of equations is equal to the number of unknowns then an approximate solution, due to data error, of the coefficients can be determined. This data error will be estimated in the Data Analysis.

The magnitude of the local gravity vector was calculated by two methods using the geographic latitude ($39^{\circ} 47' 17''$ N), longitude ($84^{\circ} 05' 45''$ W) and altitude above sea level (830ft). Method one was using the gravity model of Reference (3) which considers the earth's shape an international ellipsoid. Considering only the up component of normal gravity, the value calculated was -32.154960 ft/sec/sec. Method two was using the spherical harmonic point-mass gravity model program of Reference (4). It's value for the up component of gravity was -32.154328 ft/sec/sec. Both values are acceptable, however, method two was selected since the gravity model was generated from satellite data.

Test Procedure. The IMU sensor assembly was positioned in the six shown in Figure V-3 using the analog accelerometer

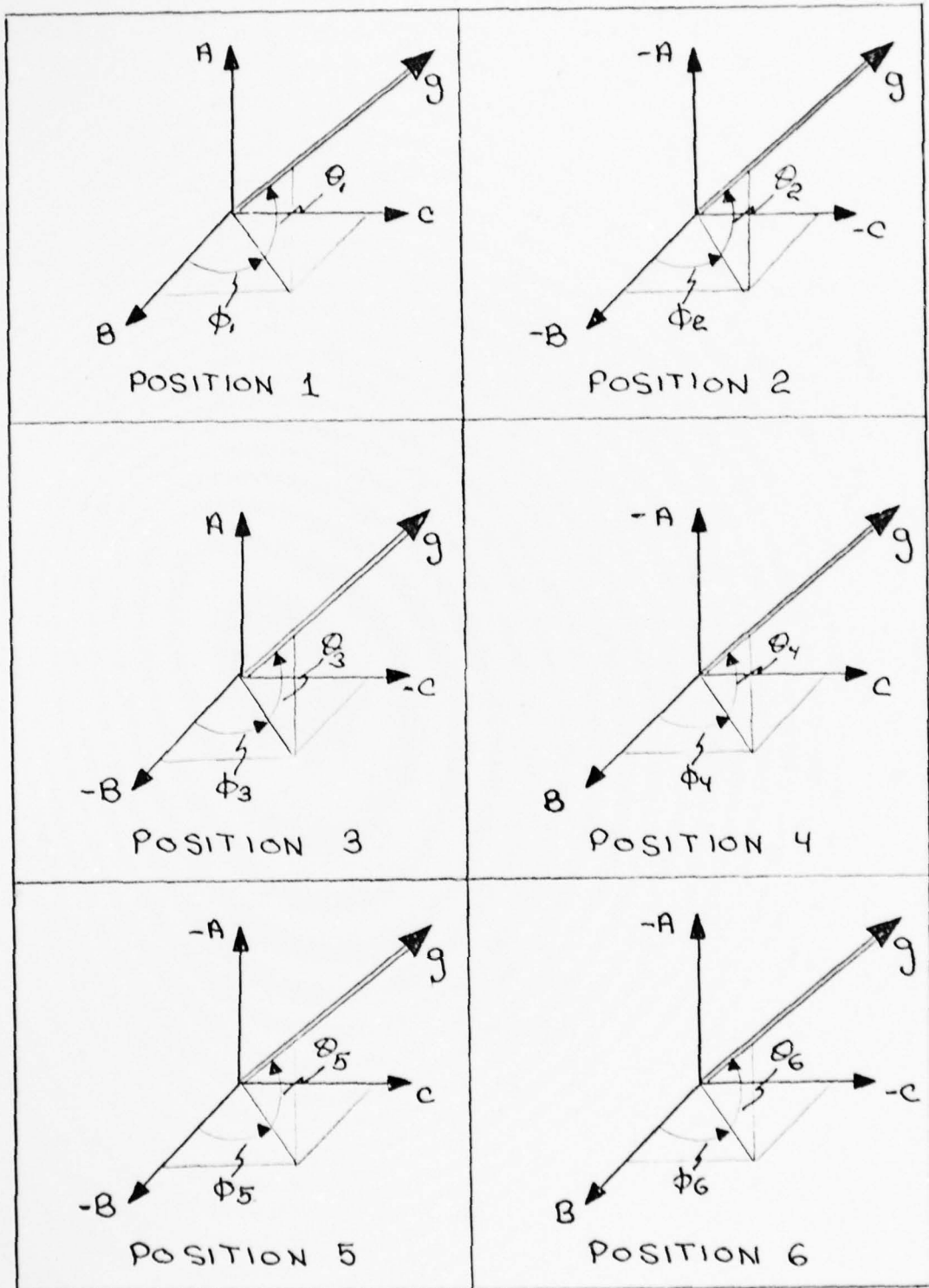


Figure V-3 Accelerometer Calibration Positions

Table V-I. Accelerometer Calibration Equations

POSITION 1:

$$A_A = K_{OA} + K_{IA} g \sin \theta,$$

$$A_B = K_{OB} + K_{IB} g \cos \theta, \cos \phi,$$

$$A_C = K_{OC} + K_{IC} g \cos \theta, \sin \phi,$$

POSITION 2:

$$A_A = K_{OA} - K_{IA} g \sin \theta_2$$

$$A_B = K_{OB} - K_{IB} g \cos \theta_2 \cos \phi_2$$

$$A_C = K_{OC} - K_{IC} g \cos \theta_2 \sin \phi_2$$

POSITION 3:

$$A_A = K_{OA} + K_{IA} g \sin \theta_3$$

$$A_B = K_{OB} - K_{IB} g \cos \theta_3 \cos \phi_3$$

$$A_C = K_{OC} - K_{IC} g \cos \theta_3 \sin \phi_3$$

POSITION 4:

$$A_A = K_{OA} - K_{IA} g \sin \theta_4$$

$$A_B = K_{OB} + K_{IB} g \cos \theta_4 \cos \phi_4$$

$$A_C = K_{OC} + K_{IC} g \cos \theta_4 \sin \phi_4$$

POSITION 5:

$$A_A = K_{OA} - K_{IA} g \sin \theta_5$$

$$A_B = K_{OB} - K_{IB} g \cos \theta_5 \cos \phi_5$$

$$A_C = K_{OC} + K_{IC} g \cos \theta_5 \sin \phi_5$$

POSITION 6:

$$A_A = K_{OA} - K_{IA} g \sin \theta_6$$

$$A_B = K_{OB} + K_{IB} g \cos \theta_6 \cos \phi_6$$

$$A_C = K_{OC} - K_{IC} g \cos \theta_6 \sin \phi_6$$

readings scaled at 1 VDC/g. These signals are obtained from the accelerometer module card (P3) of the electronics assembly. The rate-table was locked and digital data was recorded for 60 seconds in each of the six positions. The reason for selecting the 60 seconds will be discussed in Data Analysis.

Dynamic 6-Position Test

Test Description. The Dynamic 6-position test was conducted to determine the gyros bias and scale factor by positioning the IMU with respect to the rate-table axis and rotating the table at a constant rate. Earth rate was considered and rejected as a reference since rotating the rate-table at greater than or equal to 2 degrees/second was required to provide sufficient parameter sensitivity. This will be discussed in the Data Analysis.

The rate-tables axis, assuming aligned to the earth's gravity vector, was positioned with respect to the gyros as shown in Figure V-4. The angles α and β were used to define the components of rotation rate along the input axis of each

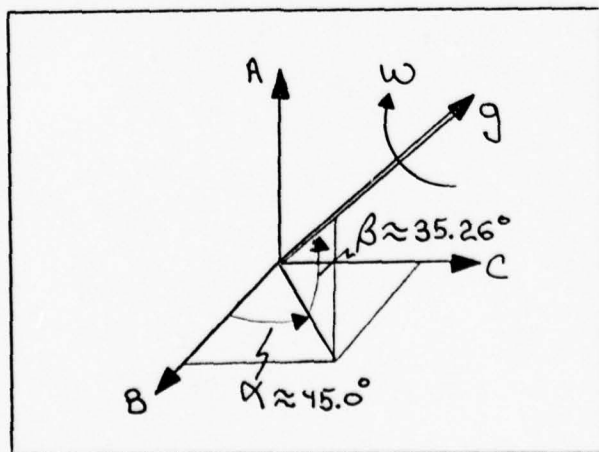


Figure V-4. Gyros Reference Position

gyro. Then rotating the rate-table at a constant rate clockwise with the angles β and α unknown the following non-linear equation were developed from model equation V-3:

$$\bar{w}_A = K_{0A} + K_{1A} w \sin \beta \quad (V-7)$$

$$\bar{w}_B = K_{0B} + K_{1B} w \cos \beta \cos \alpha \quad (V-8)$$

$$\bar{w}_C = K_{0C} + K_{1C} w \cos \beta \sin \alpha \quad (V-9)$$

With 3 equations and 8 unknowns it was required to position the IMU in the 6 positions shown in Figure V-5. This generates 18 equations with 18 unknowns as shown listed in Table V-II. Since the equations are similar to the accelerometers equations of Table V-I, an approximate solution, due to data errors, of the coefficients can be determined. This data error will also be estimated in the Data Analysis.

Test Procedure. The IMU sensor assembly was positioned in the six positions shown in Figure V-5, which is the same as the static 6-position test, using the accelerometers analog values. Data was recorded for 60 seconds in each position when the rate-table reached a constant speed of approximately 2 deg/sec. The actual rate of the table was determined by timing 180 degrees of table rotation. Also the reason for selecting 60 seconds as the data recording time and rate-table speed is discussed in Data Analysis.

Data Analysis

The data analysis was performed to determine the optimal length (integration time) of data for the static and dynamic

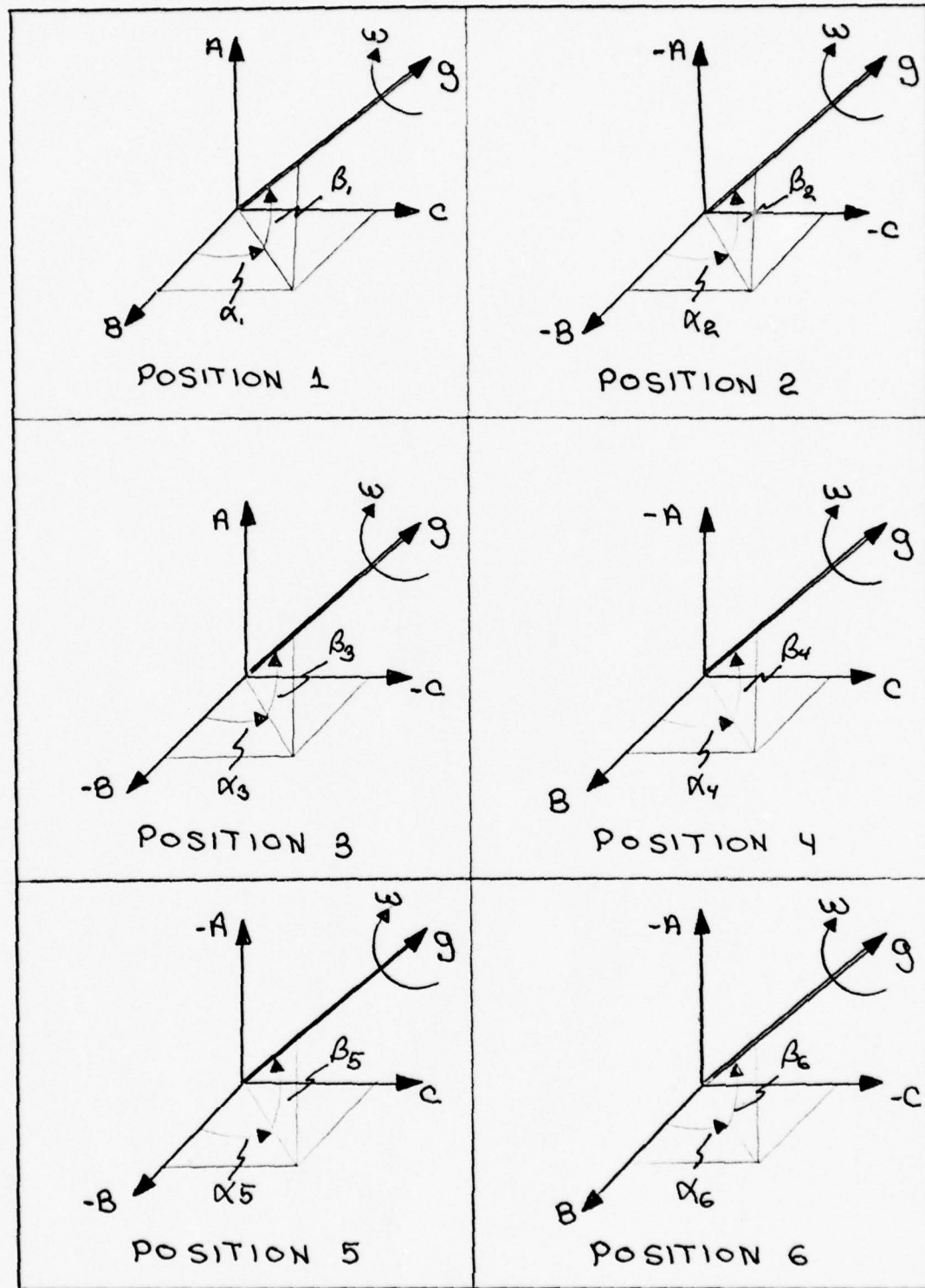


Figure V-5. Gyro Calibration Positions

Table V-II. Gyro Calibration Equations

POSITION 1:

$$W_A = K_{OA} + K_{IA} w \sin \beta_1$$

$$W_B = K_{OB} + K_{IB} w \cos \beta_1 \cos \alpha_1$$

$$W_C = K_{OC} + K_{IC} w \cos \beta_1 \sin \alpha_1$$

POSITION 2:

$$W_A = K_{OA} - K_{IA} w \sin \beta_2$$

$$W_B = K_{OB} - K_{IB} w \cos \beta_2 \cos \alpha_2$$

$$W_C = K_{OC} - K_{IC} w \cos \beta_2 \sin \alpha_2$$

POSITION 3:

$$W_A = K_{OA} + K_{IA} w \sin \beta_3$$

$$W_B = K_{OB} - K_{IB} w \cos \beta_3 \cos \alpha_3$$

$$W_C = K_{OC} - K_{IC} w \cos \beta_3 \sin \alpha_3$$

POSITION 4:

$$W_A = K_{OA} - K_{IA} w \sin \beta_4$$

$$W_B = K_{OB} + K_{IB} w \cos \beta_4 \cos \alpha_4$$

$$W_C = K_{OC} + K_{IC} w \cos \beta_4 \sin \alpha_4$$

POSITION 5:

$$W_A = K_{OA} - K_{IA} w \sin \beta_5$$

$$W_B = K_{OB} - K_{IB} w \cos \beta_5 \cos \alpha_5$$

$$W_C = K_{OC} + K_{IC} w \cos \beta_5 \sin \alpha_5$$

POSITION 6:

$$W_A = K_{OA} - K_{IA} w \sin \beta_6$$

$$W_B = K_{OB} + K_{IB} w \cos \beta_6 \cos \alpha_6$$

$$W_C = K_{OC} - K_{IC} w \cos \beta_6 \sin \alpha_6$$

6-position tests. Also the estimated data error was determined at the selected integration time to aid in solving for the coefficients of the accelerometers and gyros model equations.

The optimal data length for the calibration tests was determined by calculating the standard deviation for different integration times. This was accomplished by recording data from the IMU in a fixed position for eight minutes. Then the test data was processed from the magnetic tape for different integration times. The standard deviation computed was an unbiased estimator of the form

$$\text{Standard Deviation}(\sigma) = \left[\frac{\sum y_i^2}{(N-1)} - \frac{(\sum y_i)^2}{N(N-1)} \right] \quad (V-10)$$

where y_i is data with units of pulses per second and N is the number of data samples per integration time. The results are shown plotted in Figure V-6 for the accelerometers and Figure V-7 for the gyros. The number of data samples per integration time selected was 10 which was determined by analysis of 5,10, 15, 20, 30, and 40 samples at various integration times.

The graphs indicate an expected data trend and 60 seconds was selected as the intergration time for the calibration tests. Also since there is approximately 1000 feet of magnetic tape per reel, all six positions of the static or dynamic test can be recorded on one reel for more convenient data processing. Therefore, with 60 seconds of data recorded in each position, the estimated data error was 0.05 pulses per second for the accelerometers and 0.01 pulses per second for the gyros.

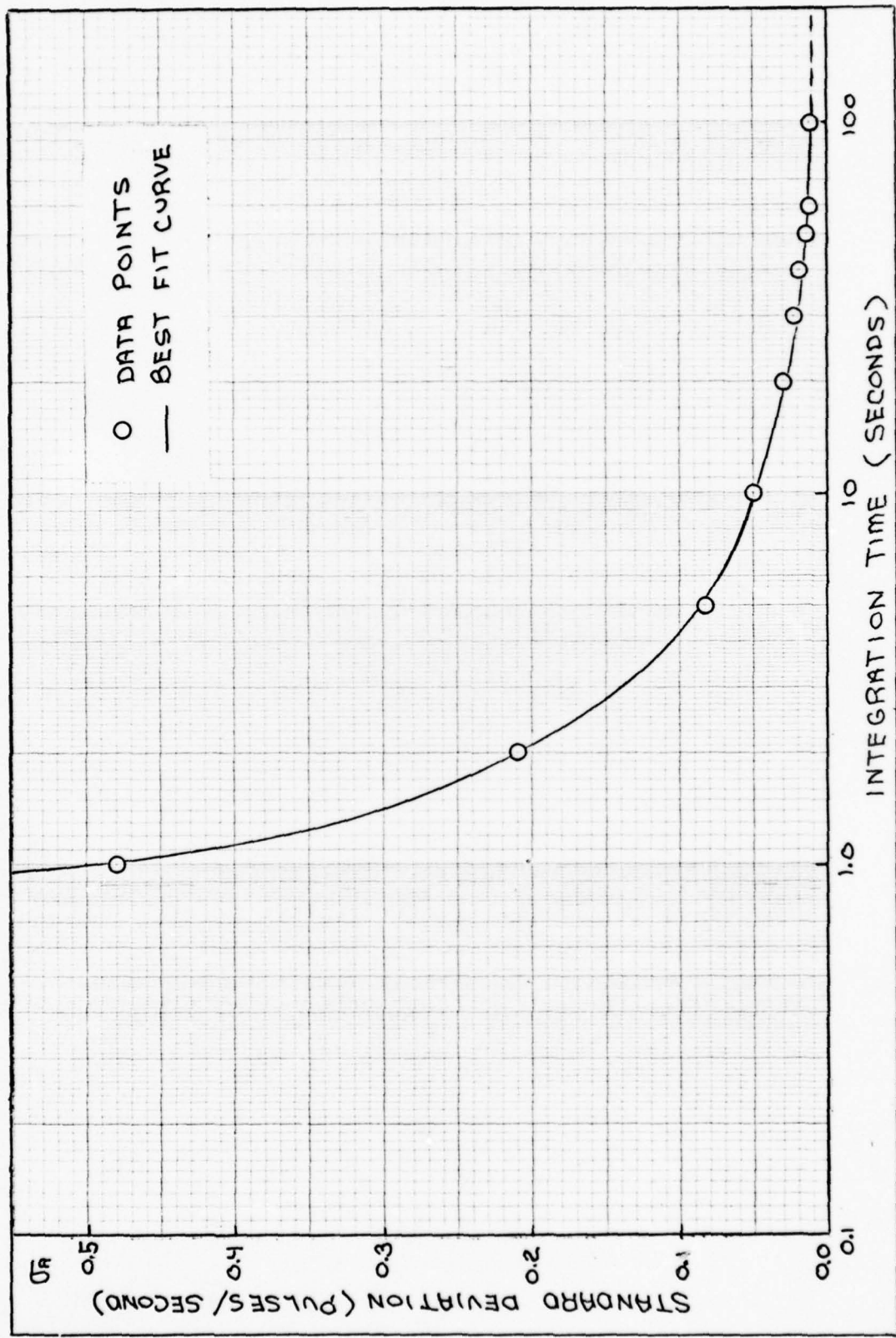


Figure V-6. Accelerometer Standard Deviation vs. Integration Time

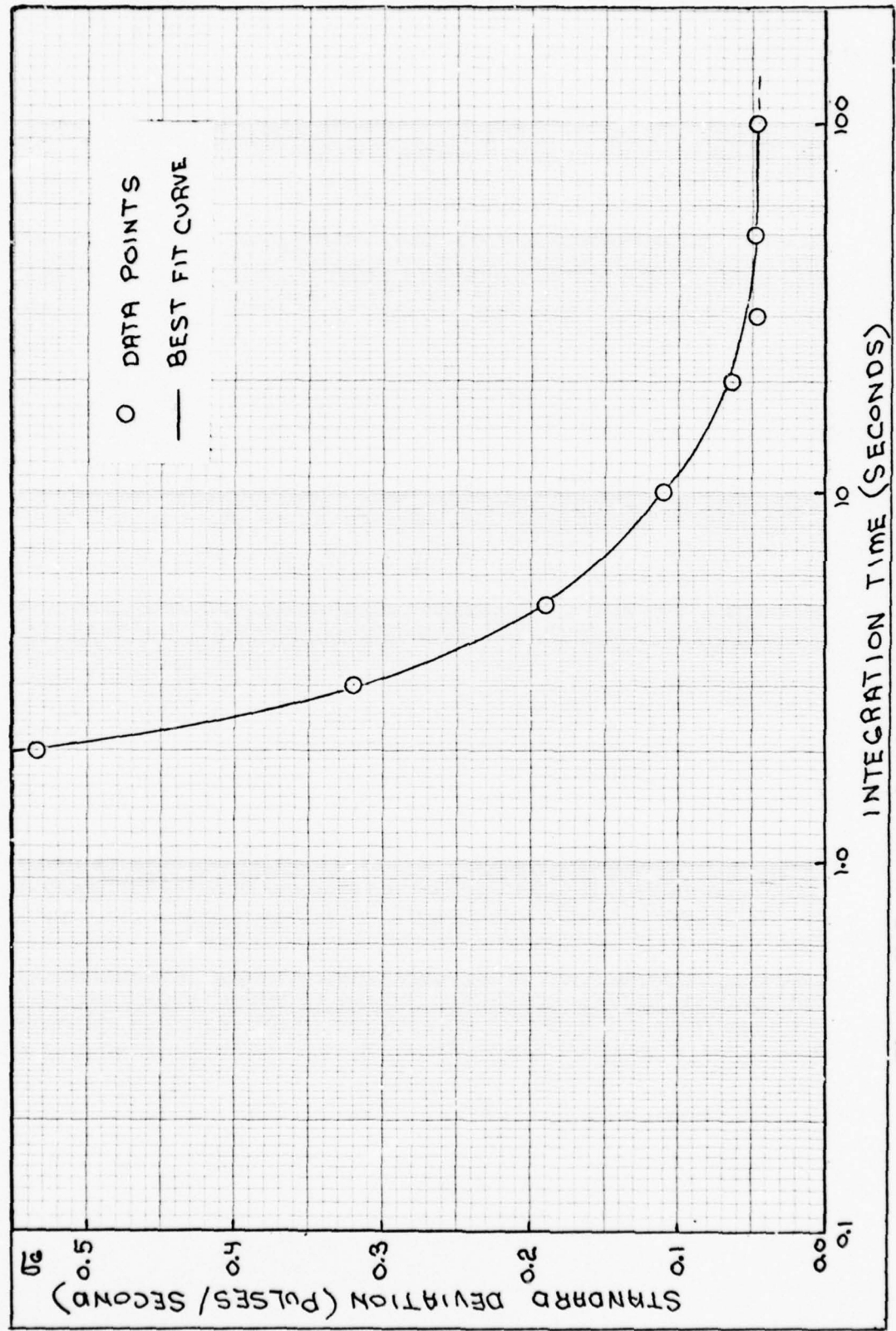


Figure V-7. Gyro Standard Deviation vs. Integration Time

The estimated error of bias and scale factor to data error was determined by analysis of the model equation. Considering the accelerometer model equation V-1, the perturbation equation can be expressed as

$$\delta A = \delta K_0 + \delta K_i f_i + \delta f_i K_i \quad (V-11)$$

which express error in accelerometer output in terms of error in bias, scale factor and input specific force. Assuming bias and scale factor are independent, and specific force error can be neglected the following analysis can be performed:

(1) assuming $\delta K_i = 0$ and $\delta A = \delta f_i$ then

$$\delta K_0 = \delta A \quad (V-12)$$

(2) assuming $\delta K_0 = 0$ and $\delta A = \delta f_i$ then

$$\delta K_i = \delta A / f_i \quad (V-13)$$

This indicates an approximate relationship (sensitivity) between the accelerometer output error and bias scale factor error.

The same analysis can be applied to the gyro model equation V-3 to obtain the perturbation equation

$$\delta \omega = \delta K_0 + \delta K_i \omega_i + \delta \omega_i K_i \quad (V-14)$$

then assuming the input rotation rate error is negligible produces the following results:

(1) assuming $\delta K_i = 0$ and $\delta \omega = \delta \omega_i$ then

$$\delta K_0 = \delta \omega \quad (V-15)$$

(2) assuming $\delta K_0 = 0$ and $\delta \omega = \sqrt{C}$ then

$$\delta K_1 = \delta \omega / \omega_i \quad (V-16)$$

This indicates an approximate relationship between the gyro output error and bias or scale factor error. Figure V-8 is a plot of scale factor error for different rotation rates using equation V-16. The graph indicates scale factor error is decreased by applying a rotation rate greater than earth rate (15.041067 sec/sec). This is the reason the dynamic test, with a rate greater than or equal to 2 deg/sec, was selected for the gyro calibration sequence.

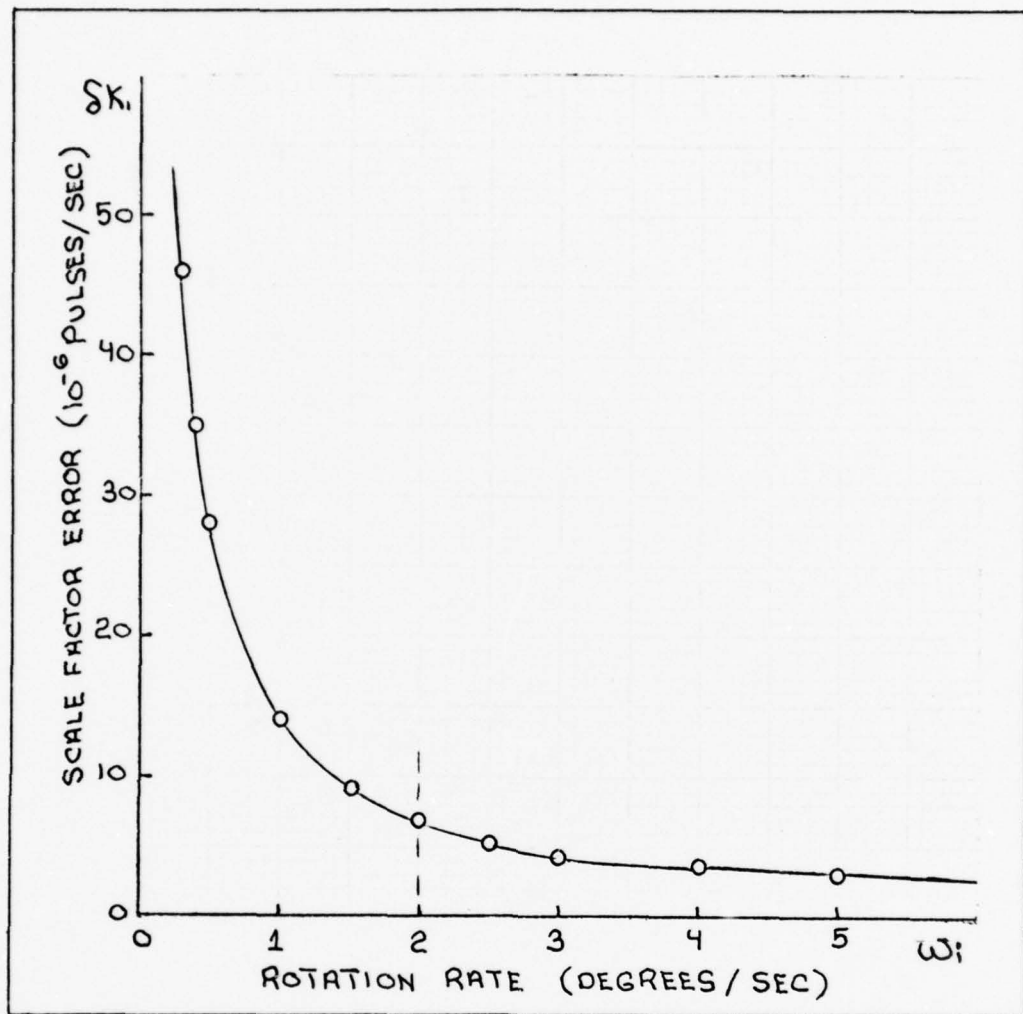


Figure V-8. Gyro Scale Factor Error vs. Rotation Rate

VI. Results and Recommendations

Results

The initial requirement was to set-up the inertial measurement unit (IMU) on the Genisco rate-table and record meaningful sensor data on magnetic tape. This effort was accomplished by designing a test fixture, the data monitor controller, multiplexer, and programmer. The test fixture allowed the capability to position the IMU sensor assembly in any desired orientation. The data monitor controller, a modified Sperry design, was required to control the operation of the IMU to obtain digital data in the absence of a computer. The multiplexer buffered and multiplexed the digital data to interface with a Cipher magnetic tape recorder. The programmer was needed to control the functions of the tape recorder due to the requirements of the IMU data sampling rate and the read capabilities of the CDC 6600 digital computer. Chapter V discusses the above effort in more detail.

The next requirement was to process the data recorded on the magnetic tape. This required the development of a FORTRAN program to process the recorded binary data and output the data from each instrument in a desired usable format. The program involved a search routine for an octal code word (4444) attached to each data group by the multiplexer. Once the code is located the data is sorted and converted from binary to a numerical value for each instrument. Chapter IV discusses the functions of the program in more detail and Appendix B is a listing of the program with comments throughout to aid other users.

The final requirement was to determine the bias and scale factors for the laser gyros and accelerometers. This was to be accomplished by the calibration test developed in Chapter V. The dynamic 6-position test for the gyros was not completed due to a problem with gyro "A". This gyro would not respond to any rotation rates from the rate-table thus, the output data required to solve for the gyros coefficients was not available.

The static 6-position test for the accelerometers was completed and the output data (Table VI-I) was processed for integration time of 60 seconds. This data and the local gravity magnitude (32.154328 ft/sec/sec) was used with an AFIT subroutine (NS01A) to solve the system of nonlinear calibration equations of Table V-I. The best results obtained by the routine is shown in Table VI-II to an accuracy of approximately 0.75 pulses/second. The desired accuracy was 0.01 pulses/second, which was determined from the data analysis shown in Figure V-6.

A sample problem was developed to initially verify the routines capability with the calibration equations. Gaussian random numbers with a 0.01 standard deviation was applied to the sample problem data. The estimated solutions were obtained to the desired accuracy which validated the routines capability. Therefore, the accelerometer model equation was determined to be inadequate for the test data and a higher order model must be considered.

Recommendations

Several recommendations can be made for further work. One is to develop a more adequate model for the accelerometers.

This would include non-linearities and a different approach to determine the additional coefficients. Also the dynamic 6-position test for the gyros should be completed when the problem with gyro "A" is corrected.

A microprocessor, if available, could be interfaced with the electronic assembly to control the IMU operation. This operation can be divided into four phases as follows:

- (1) Initial start up
- (2) Warm-up
- (3) Checkout and Calibration
- (4) Navigation

which are described in more detail in Reference (1). Also the microprocessor would allow more efficient storage of IMU data on magnetic tape by online processing before recording.

Table VI-I. Accelerometer (Static) Test Data

POSITION 1	
$A_A = -441.633333$ Pulses/Second	↓
$A_B = -442.166667$	↓
$A_C = -442.466667$	↓
POSITION 2	
$A_A = 442.533333$ Pulses/Second	↓
$A_B = 443.300000$	↓
$A_C = 442.900000$	↓
POSITION 3	
$A_A = -431.933333$ Pulses/Second	↓
$A_B = 446.550000$	↓
$A_C = 445.966667$	↓
POSITION 4	
$A_A = 451.816667$ Pulses/Second	↓
$A_B = -436.833333$	↓
$A_C = -436.700000$	↓
POSITION 5	
$A_A = 447.350000$ Pulses/Second	↓
$A_B = 447.050000$	↓
$A_C = -433.050000$	↓
POSITION 6	
$A_A = 445.311111$ Pulses/Second	↓
$A_B = -432.588889$	↓
$A_C = 445.644444$	↓

Table VI-II. Accelerometer Calibration Equation Solutions

SCALE FACTORS(FT/SEC/PULSE)		
	•233•8940E+02	•23369218E+02
BIAS(PULSES/SEC)		
	•46637044E+00	•56486562E+00
POSITION ANGLES(RADIANS)		
	•61341945E+00	•76764319E+00
	•51780878E+00	•75705641E+00
	•60005849E+00	•75687653E+00
	•62905337E+00	•76706466E+00
	•62116512E+00	•75252828E+00
	•62042114E+00	•78091414E+00
POSITION ANGLES(DEGREES)		
	•35146351E+02	•43982721E+02
	•35168657E+02	•43949101E+02
	•34381395E+02	•43938913E+02
	•36042395E+02	•43956732E+02
	•36390145E+02	•43122470E+02
	•35247518E+02	•4745383E+02
RESIDUALS		
	•65150423E+00	
	•62209535E+00	
	•58131247E+00	
	-•37467905E+00	
	-•49668337E+00	
	-•48472230E+00	
	-•63782452E+00	
	•56947559E+00	
	•60321131E+00	
	-•15027783E+00	
	-•25201702E-01	
	-•60595052E-02	
	-•59169300E+00	
	-•47842394E+00	
	•48323905E+00	
	•97736753E+00	
	-•10642268E+01	
	•97907335E+00	
ACC	7.	
DSTEP	.0001	

Bibliography

1. Sperry Report No. 60720-1. Operation and Service Manual, Sperry Inertial Measurement Unit, Part No. 4331-704792. Revision B. Great Neck, New York: Sperry Gyroscope, 27 Feb. 1976.
2. Cipher Data Products-100. Operation and Maintenance Manual for the Model 85H Magnetic Tape Recorder. San Diego, Calif: Cipher Data Products, Jan 1969.
3. Windall, William S. and Grundy, Peter A. Inertial Navigation System Error Models. Holloman AFB, New Mexico: Guidance Test Division, 6585th Test Group, 11 May 1973. (AD-912-489L)
4. Smart, Richard W. Spherical Harmonic Point-Mass Gravity Model Program. Unpublished Report. Wright-Patterson AFB, Ohio: Air Force Institute of Technology, August 1978.
5. Engineering Staff of the Texas Instruments Inc. The TTL Data Book for Design Engineers. First Edition. Dallas, Texas: Texas Instruments Inc., 1973.
6. Sundstrand Data Control. Q-Flex Servo Accelerometers for Strapdown Inertial Guidance Systems. Redmond, Washington: Sundstrand Data Control Inc., (undated).
7. Sapp, William F. and Messmer, John B. Developmental Investigation of Bell Aerosystems Model IX Accelerometer. Report No. NADC-AM-7010. Warminster, Pa: Department of the Navy, Naval Air Development Center Johnsville, 4 Nov 1970. (AD-877494)
8. Sperry Report No. 4284-20104-1. Sperry Model A SLG-15 Laser Gyro Operation, Service and Performance Manual. Great Neck, New York: Sperry Gyroscope, Nov 1974. (AD-B004888L)
9. Wrigley, Walter, Hollister, Walter M. and Denhard, William G. Gyroscope Theory Design and Instrumentation. Cambridge, Massachusetts: The M.I.T. Press, 1996.
10. SGD 20229-1. Engineering Services for Recalibration of Sperry SLIC-15 Inertial Measurement Unit, Serial No. 002, for Air Slew Maneuver Tests. Great Neck, New York: Sperry Gyroscope Division, Feb 1977.

Appendix A
Schematic Diagrams and Parts List

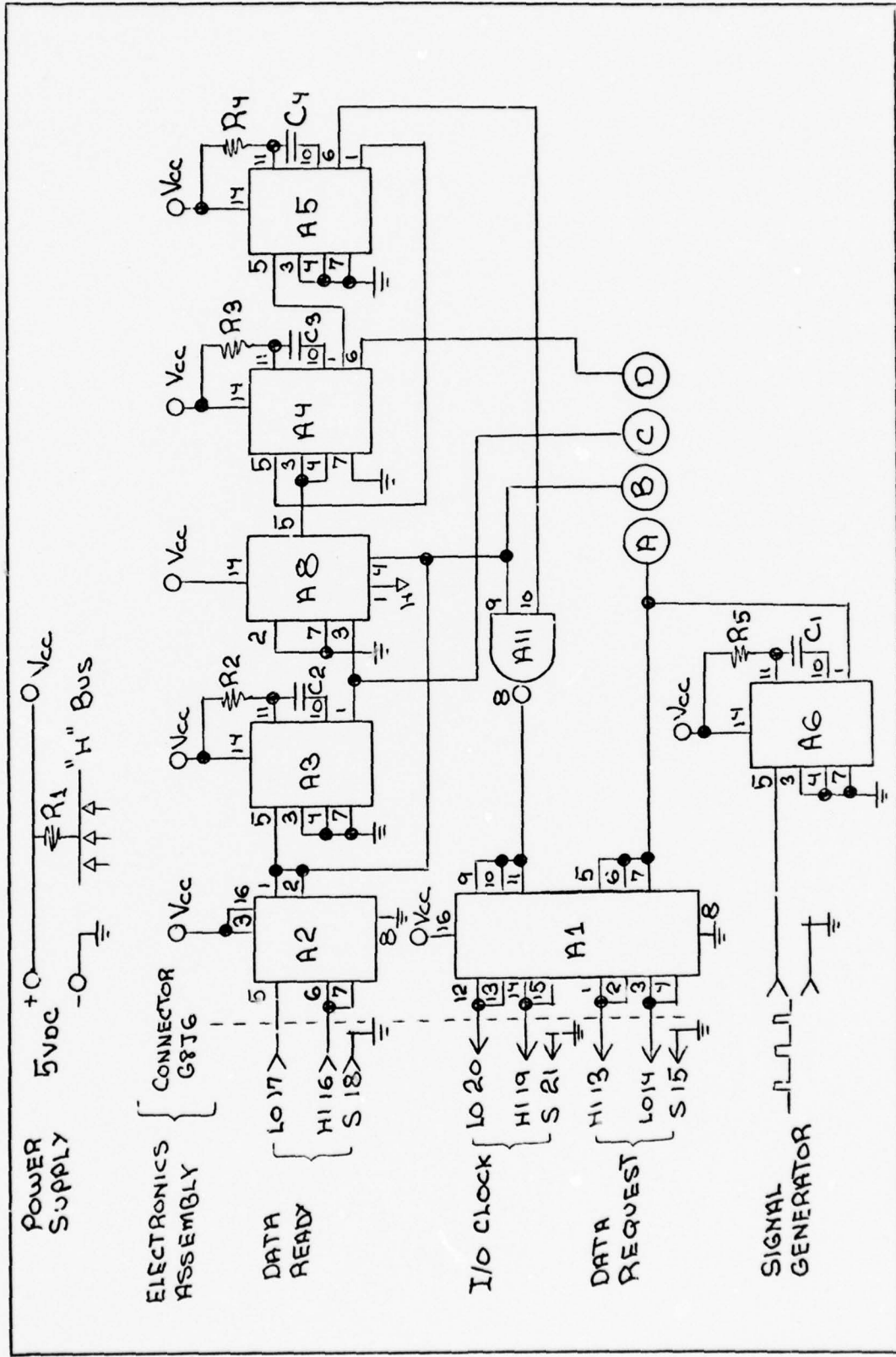


Figure A-1. Data Monitor Controller Schematic 1 of 2

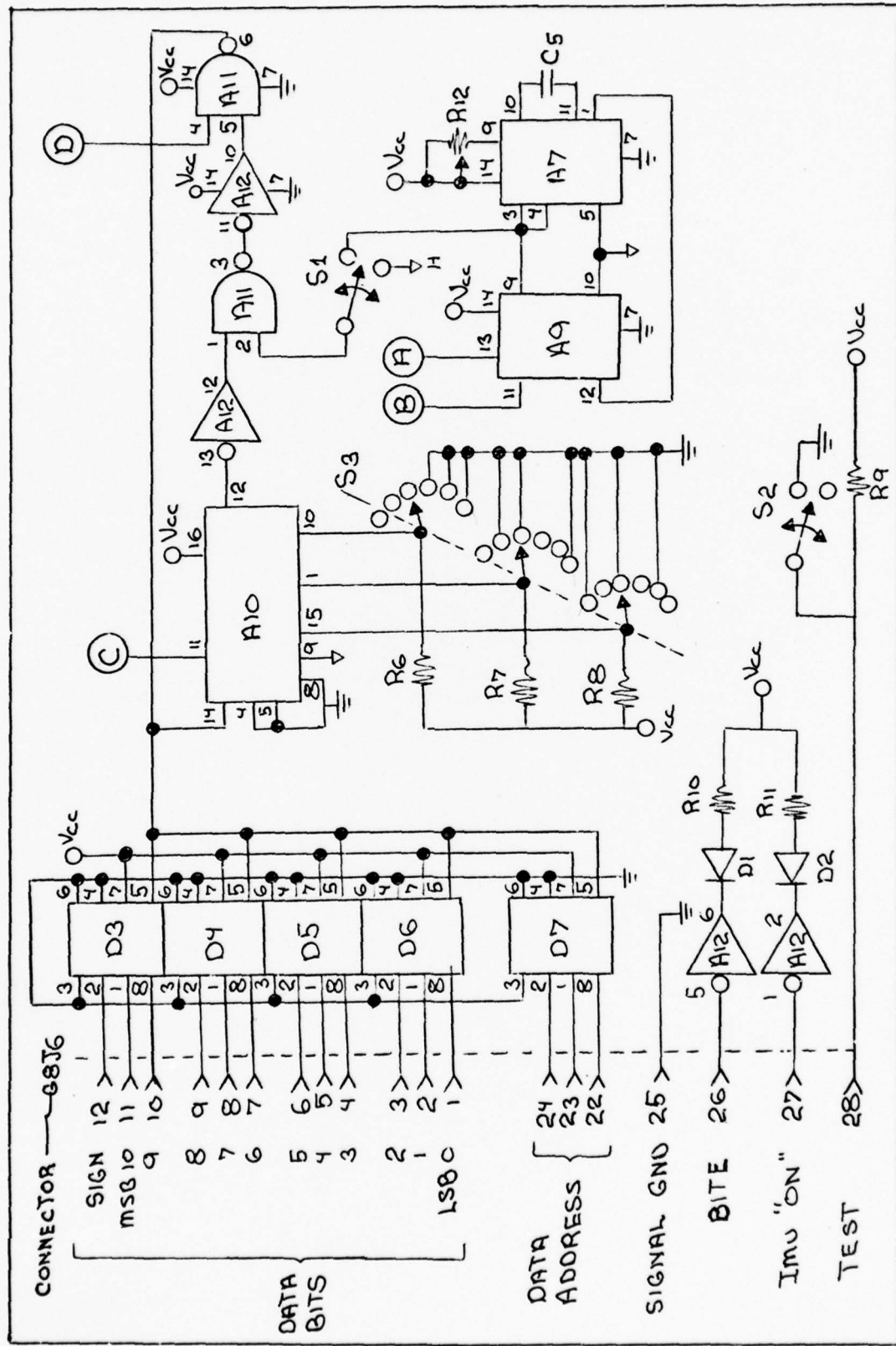


Figure A-2. Data Monitor Controller Schematic 2 of 2

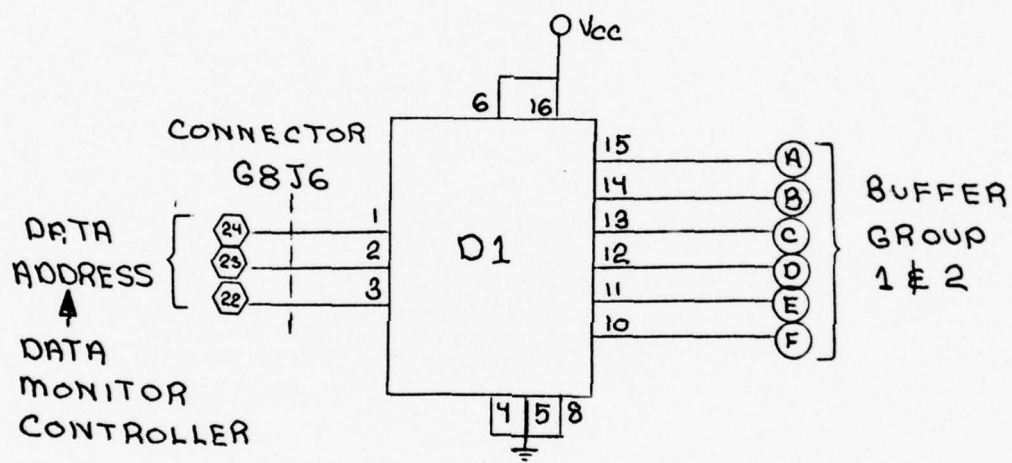


Figure A-3. Multiplexer Schematic(Decoder) 1 of 6

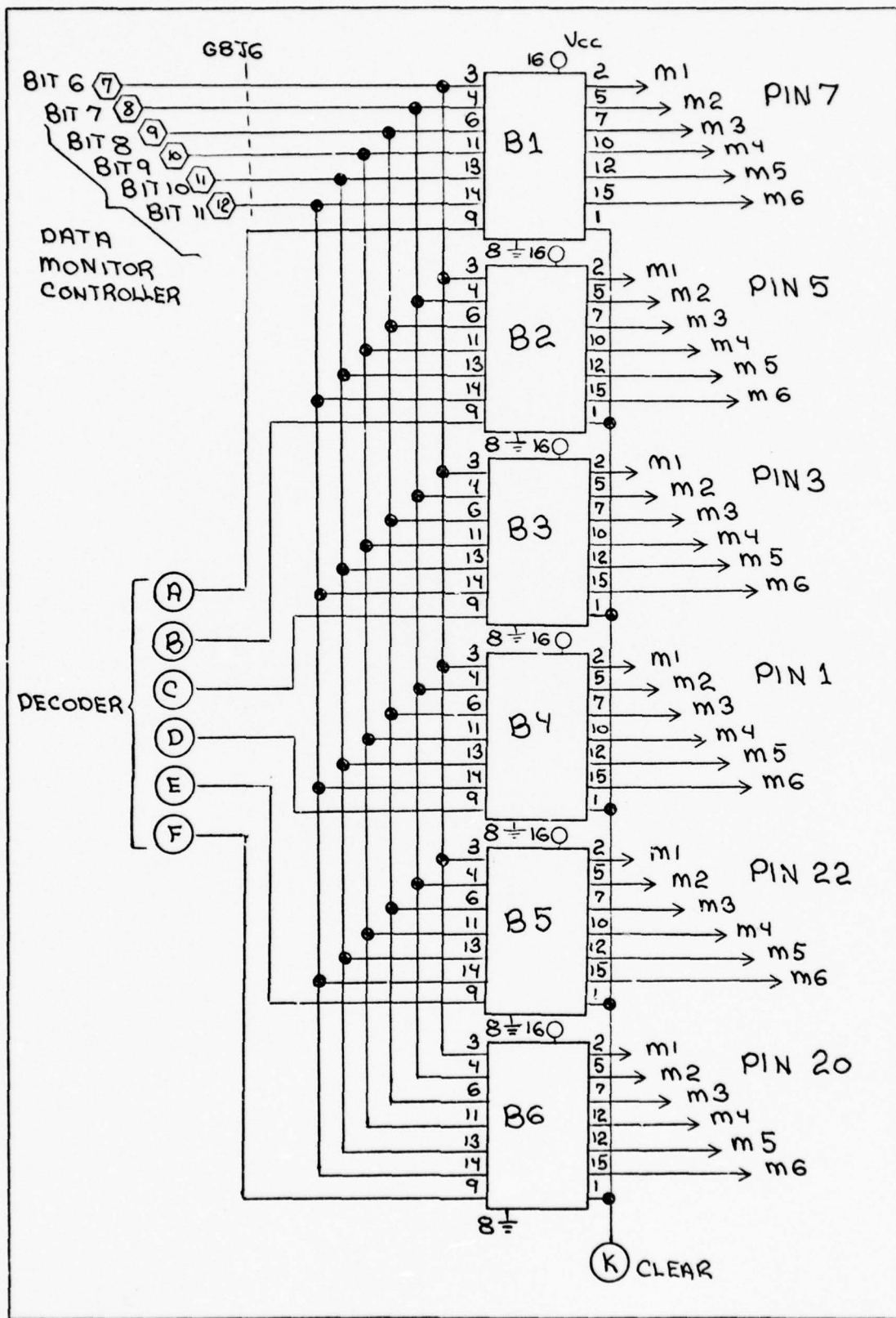


Figure A-4. Multiplexer Schematic (Buffer Group #1) 2 of 6

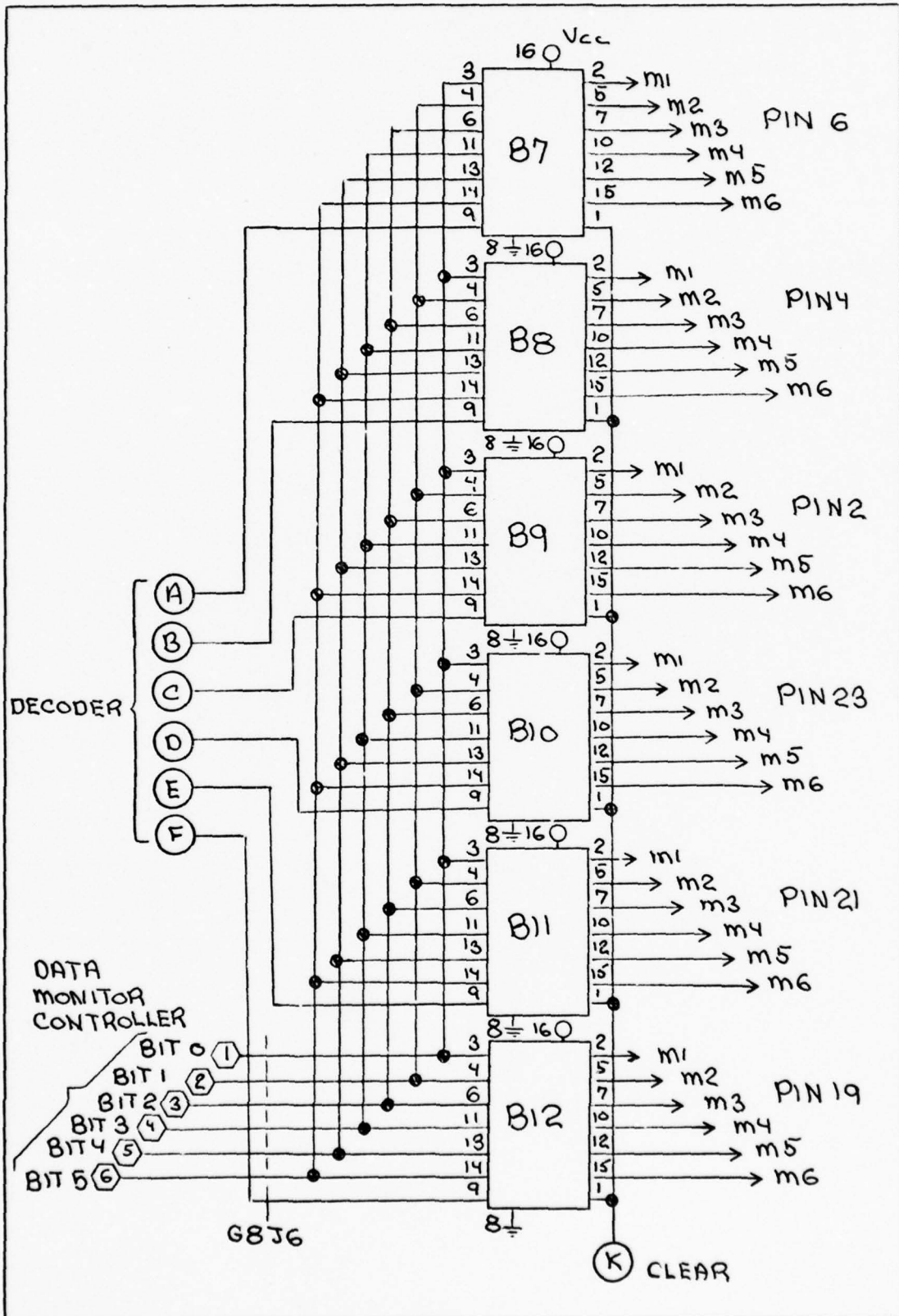


Figure A-5. Multiplexer Schematic(Buffer Group#2) 3 of 6

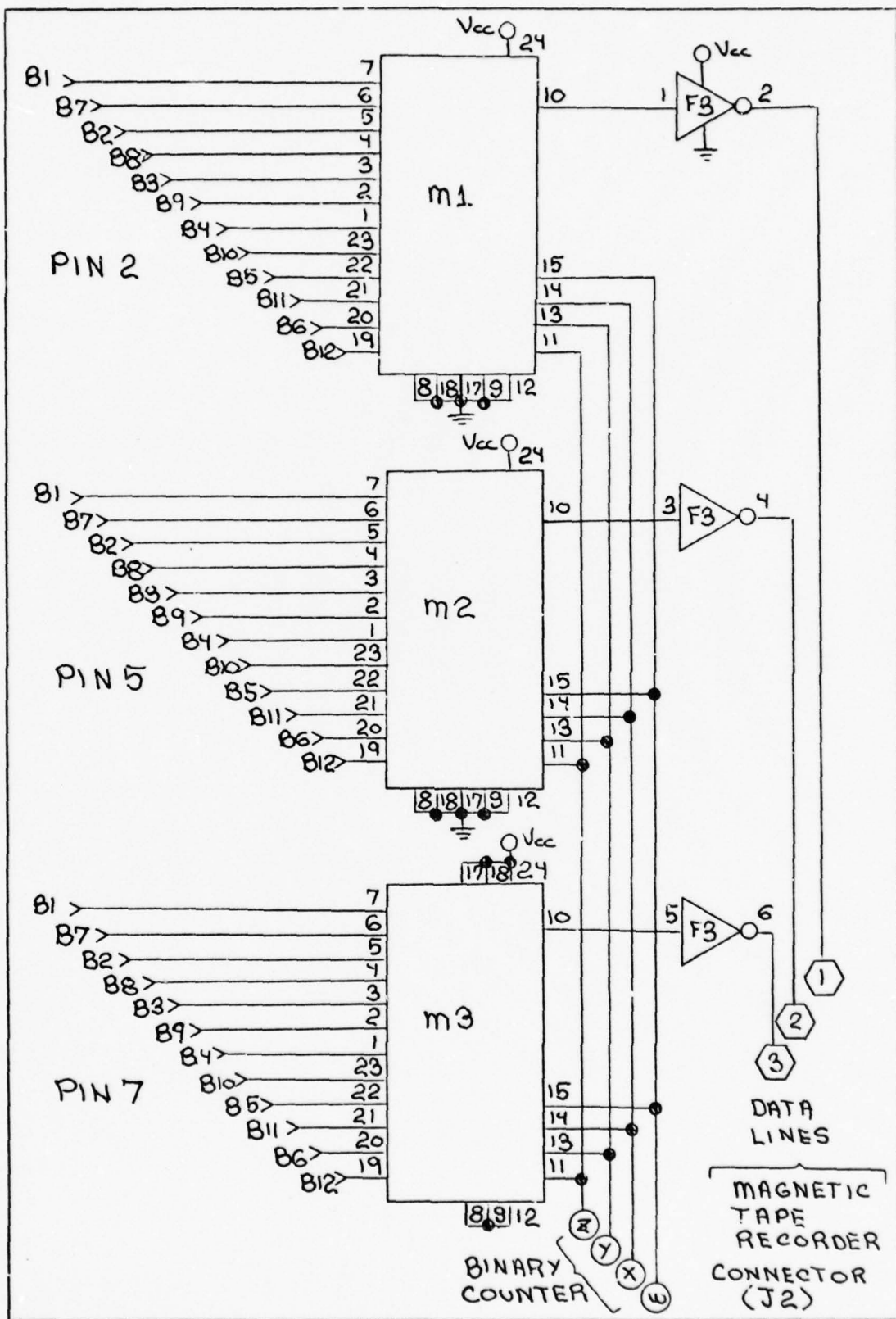


Figure A-6. Multiplexer Schematic (Mux Group#1) 4 of 6

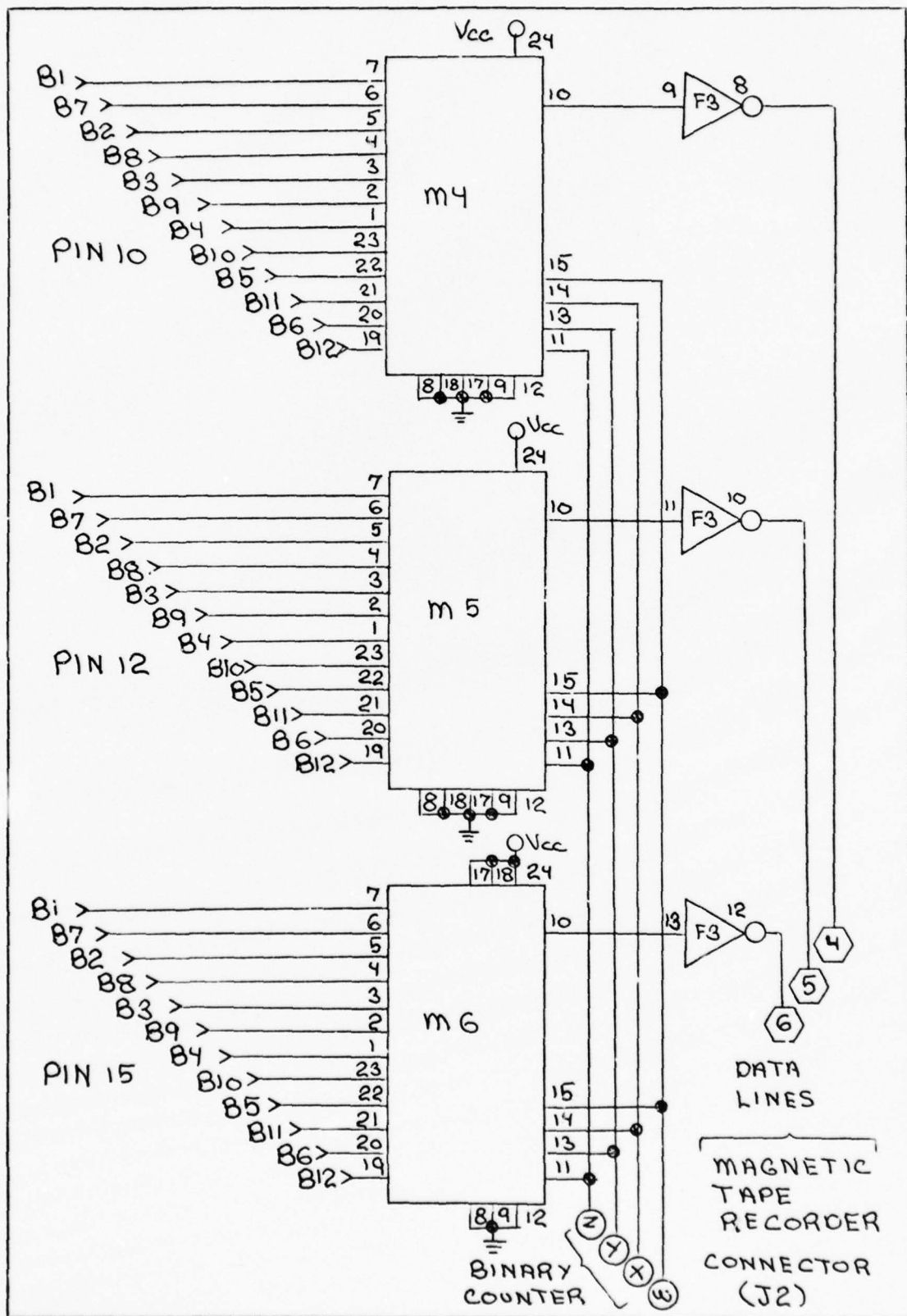


Figure A-7. Multiplexer Schematic (Mux Group #2) 5 of 6

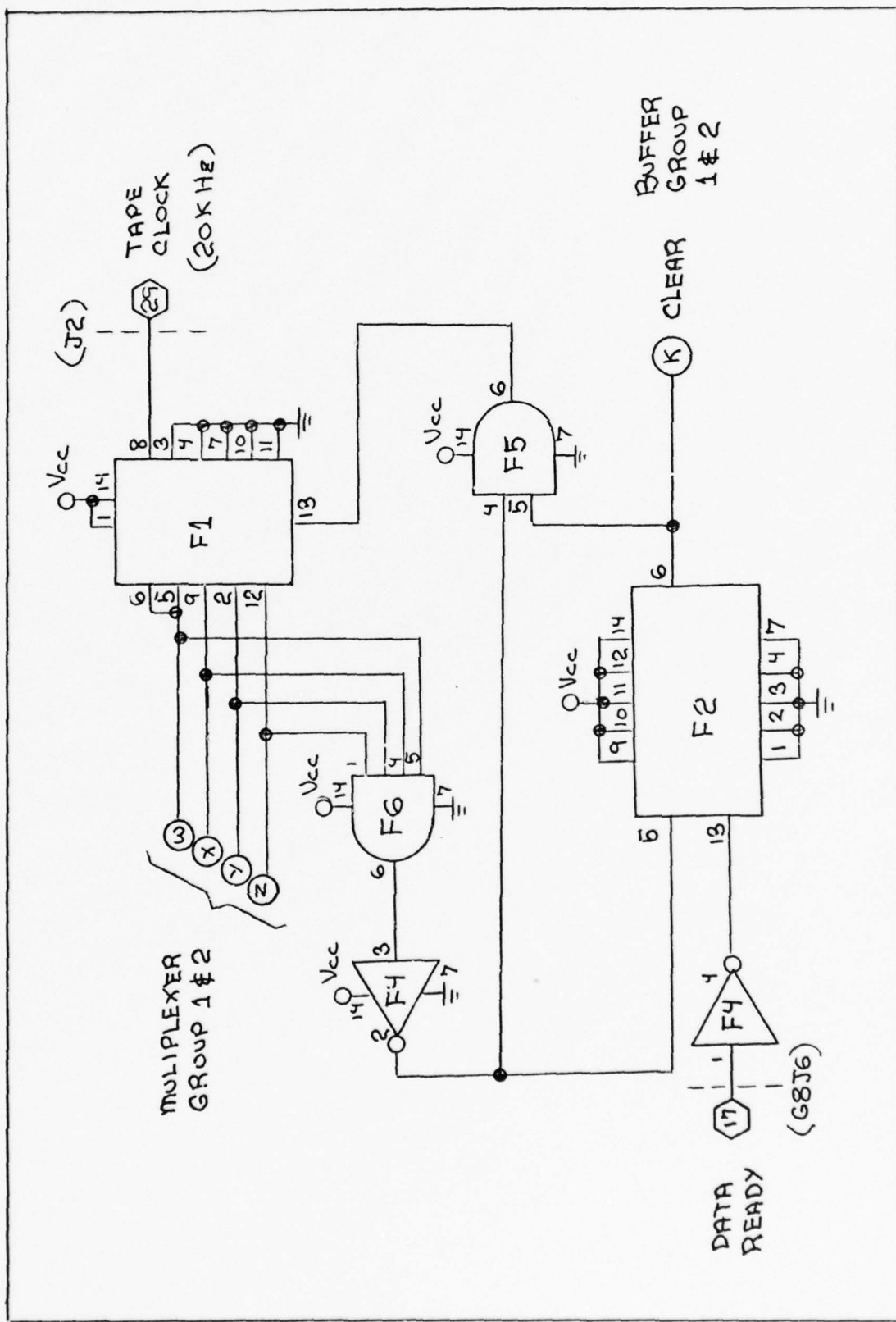


Figure A-8. Multiplexer Schematic (Binary Counter) 6 of 6

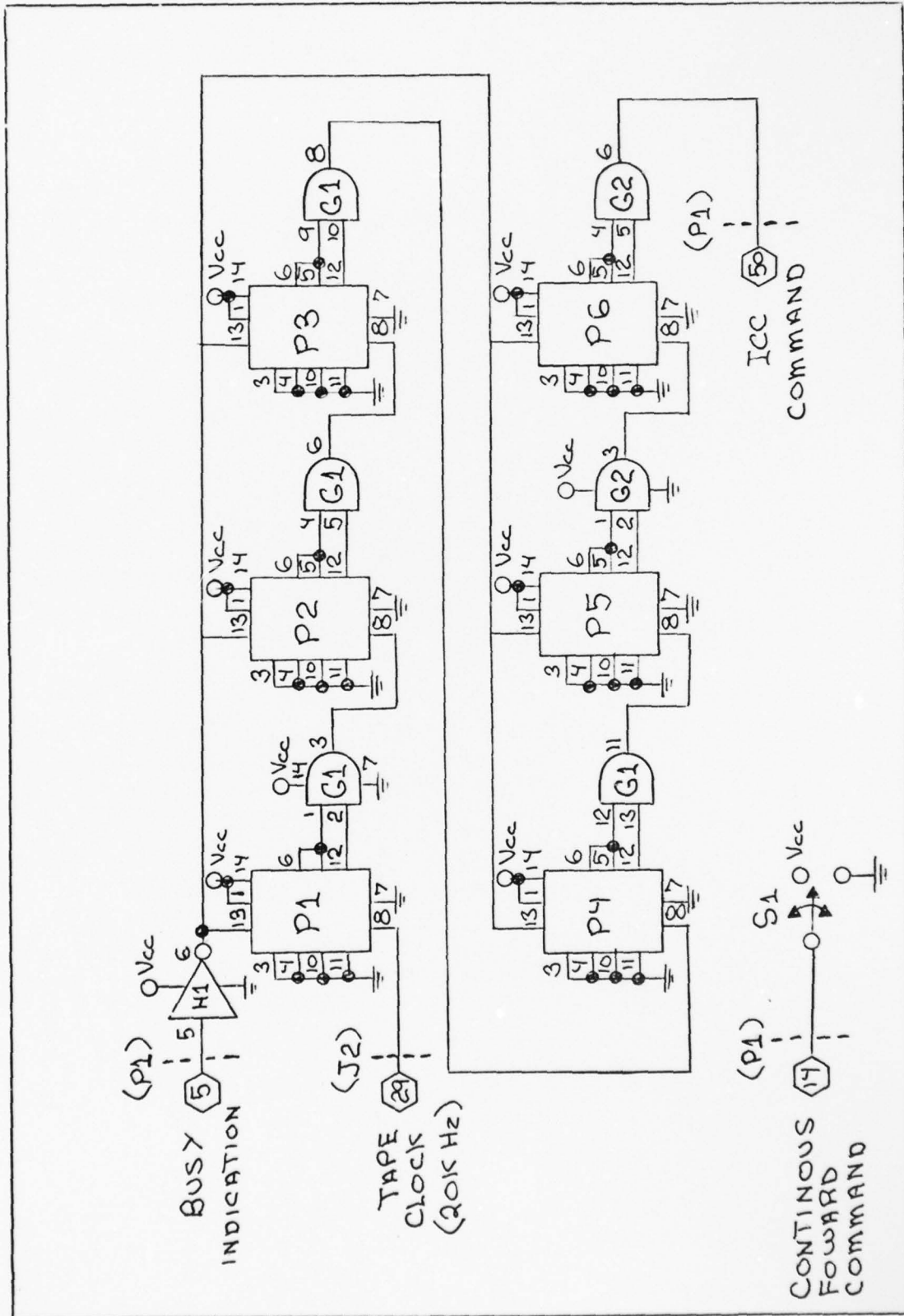


Figure A-9. Programmer Schematic

Table A-I. Data Monitor Controller Parts Listing

SCHEMATIC PARTS LIST		
Data Monitor Controller		
Ref Desig	Description	Part Number
C1	Capacitor	100pf
C2		1000pf
C3		1000pf
C4		100pf
C5		100pf
R1	Resistor	1K ohms
R2		6.8K
R3		6.8K
R4		3.3K
R5		3.3K
R6		4.7K
R7		4.7K
R8		4.7K
R9		4.7K
R10		240
R11		240
R12	Resistor, Variable	50K
D1	LED	
D2	LED	
D3	LED Display	HP 5082-7340
D4		

Table A-I. (Cont.)

SCHEMATIC PARTS LIST		
Data Monitor Controller		
Ref Desig	Description	Part Number
D5	LED Display	HP 5082-7340
D6		
D7		
S1	Switch, Toggle	SPST
S2	Switch, Toggle	SPST
S3	Switch, Rotary	3P-6POS
A1	Dual Line Driver	9614
A2	Dual Line Receiver	9615
A3	Monostable Multivibrator	SN74S121
A4		
A5		
A6		
A7		
A8	Dual D-Type Flop-Flop	SN74S7474
A9		
A10	Up/Down Binary Counter	SN74S191
A11	Quad 2-Input NAND Gate	SN74S7400
A12	Hex Inverter	SN74S7404

Table A-II. Multiplexer Parts Listing

SCHEMATIC PARTS LIST		
Multiplexer		
Ref Desig	Description	Part Number
D1	Decoder/Demultiplexer	SN74S138
B1	Hex/Quadruple D-Type Flip-Flops	SN74S174
B2		
B3		
B4		
B5		
B6		
B7		
B8		
B9		
B10		
B11		
B12		
M1	Data Selectors/Multiplexers	SN74150
M2		
M3		
M4		
M5		
M6		
F1	Binary Counter	SN74LS197
F2	J-K Flip-Flops	SN74101

Table A-II. (Cont.)

SCHEMATIC PARTS LIST		
Multiplexer		
Ref Desig	Description	Part Number
F3	Hex Inverters	SN7404
F4	Hex Inverters	SN7404
F5	Quad 2-Input AND Gates	SN7409
F6	Dual 4-Input AND Gates	SN7421

Table A-III. Programmer Parts Listing

SCHEMATIC PARTS LIST

Programmer		
Ref Desig	Description	Part Number
P1	Binary Counters	SN74176
P2		
P3		
P4		
P5		
P6		
G1	Quad 2-Input AND Gates	SN7408
G2		
H1	Hex Inverter	SN7404
S1	Switch, Toggle	SPST

Appendix B
Computer Program Listing


```

C***** CLEAR INPUT BUFFER ****
DO 50 I=1,20000
50 A(I)=00000000000000000000000000000000
C***** BUFFER IN TAPE RECORDS & FILES ****
40
      PRINT*, ""
      BUFFER IN(1,1) (A(1),A(20000))
      IF (UNIT(1)) 65,75,75
      F5 K=LENGTH(1)
      PRINT*, " RECORD ", NN, " LENGTH ", <, " FILE ", NN
      NN=NN+1
      GO TO 60
75 K=LENGTH(1)
      PRINT*, " RECORD ", NN, " LENGTH ", <, " END OF FILE ", NN
      NN=NN+1
50
      MY=1
C***** CONTINUE ****
      GO CONTINUE
      IF (JADD.EC.10) PRINT*, " UNITS(PULSESES/0.1SEC) "
      IF (JADD.EC.110) PRINT*, " UNITS(PULSESES/SEC) "
      IF (JADD.EC.1000) PRINT*, " UNITS(PULSESES/10SEC) "
      PRINT*, ""
      PRINT 110
110 FORMAT( 21X "GVR0", T54, "ACCELEROMETER", / 9X"(A)", T22, "(B)", ,
+ T7L "(C)", T46, "(A)", T56, "(B)", T70, "(C)" )
      P1=00000000000000000000000000000000
      B2=A(1)
      R3=A(2)
      K=36
      TI=1
      JJ=1
      65
      CALL SORT(E,B1,32,93,K)
      CALL ASSIGN(E,F)
      IF (IAND.EC.1) WRITE(6,700) (F(I),I=1,6)
      DO 70 I=1,6
      70 N(1, JJ)=F(T)
      DO 10 J=4,20000

```



```

1      SUBROUTINE SORT(E,B1,B2,B3,KSTART)
C*   ****
C*   GYRO & ACCELEROMETER DATA SORTING SUBROUTINE
C*   ****
C*   B3 - WORD IN WHICH CODE(4444) IS -UPDATED
C*   P2 & P1 - WORDS PRIORITY TO B3
C*   KSTART - BIT LOCATION OF CODE(+444) IN B3
C*   D - WORKING ARRAY OF DIMENSION (12)
C*   F - SORTED DATA ARRAY OF DIMENSION(5)
C*   E(1)=ACCEL(0)   E(2)=ACCEL(1)   E(3)=ACCEL(2)
C*   E(4)=GYRO(0)   E(5)=GYRO(1)   E(6)=GYRO(2)
C*   ****
C*   ****
C*   DIMENSION D(12),E(6)
C*   INTEGER A,E,B1,B2,B3,C,D,E,F
C*   K=KSTART+12
C*   J=1
C*   IF (V.EQ.60) GO TO 55
C*   IF (V.EQ.66) GO TO 15
C*   IF (V.EQ.72) GO TO 5
C*   DO 15 I=K,60,5
C*   A=SHIFT(MASK(5),I).AND.B3
C*   K1=K1-1
C*   D(J)=SHIFT(A,K1)
C*   J=J+1
C*   IF (I.EQ.60) GO TO 15
C*   10 CONTINUE
C*   ****
C*   5   K=12
C*       GO TO 25
C*   15 K=6
C*   25 DO 26 L=K,60,5
C*   ****

```

```

35 R=SHIFT(MASK(5),L).AND.92
K2=6-L
D(J)=SHIFT(R,K2)
J=J+1
IF (J.EQ.13) GO TO 45
IF (L.EQ.6) GO TO 35
20 CONTINUE
C * * * * *
35 DO 30 M=F,60,5
C=SHIFT(MASK(5),M).AND.31
K3=6-M
D(J)=SHIFT(C,K3)
45
J=J+1
IF (J.EQ.13) GO TO 45
30 CONTINUE
C * * * * *
45 I=2
J=1
DO 40 N=1,5
F=SHIFT(D(I),5)
E(I)=D(J).OR.F)
IF (I.EQ.12) GO TO 55
I=I+2
J=J+2
40 CONTINUE
55 RETURN
END
60

```

```

1      SUBROUTINE ASSIGN (E,F)
2      C*      BINARY TO INTEGER DATA ASSIGNING SUBROUTINE
3      C*      SIGN + TWO'S COMPLEMENT
4      C*      GYRO DATA (11 BITS + SIGN)
5      C*      ACCEL DATA (6 BITS + SIGN)
6      C*      E = SORTED DATA ARRAY (SORT SUBROUTINE)
7      C*      F = ASSIGNED INTEGER VALUE DATA ARRAY OF DIMENSION (6)
8      C*      F(1)=GYRO(A)   F(2)=GYRO(B)   F(3)=GYRO(C)
9      C*      F(4)=ACCEL(A)  F(5)=ACCEL(B)  F(6)=ACCEL(C)
10
11      C*      ****
12      C*      DIMENSION E(6),F(5)
13      C*      INTEGER A,E,F,G
14      C*      J=6
15      DO 16  I=1,6
16      N=00000000000000000000000000000000
17      N=SHIFT(MASK(I),12).AND.E(J)
18      IF ((N.EQ.0).AND.(J.GE.4)) GO TO 5
19      IF ((N.EQ.0).AND.(J.LT.4)) GO TO 15
20      IF ((N.NE.0).AND.(J.LT.I)) GO TO 25
21      G=SHIFT(MASK(11),11).AND.E(J)
22      F(I)=G
23      GO TO 20
24      C*      **** GYRO (-) ****
25      G=SHIFT(MASK(5),11).AND.E(J)
26      F(I)=-2048+G
27      GO TO 20
28      C*      **** ACCELEROMETER (-) ****
29      15 A=SHIFT(MASK(6),11).AND.E(J)
30      A=SHIFT(A,-5)
31      F(I)=-64+A
32      GO TO 20
33      C*      **** ACCELEROMETER (+) ****
34      25 A=SHIFT(MASK(5),11).AND.E(J)
35      A=SHIFT(A,-5)
36      F(I)=A
37      GO TO 20
38      20 J=J-1
39      16 CONTINUE
40      RETURN
41

```


VITA

Robert Stephen Lawrence was born on 25 October 1947 in Kingston, Pennsylvania. He graduated from high school in Dallas, Pennsylvania in 1965 and attended Penn State University from which he received the degree of Bachelor of Science in Electrical Engineering in June 1970. He then attended Officer Training School, from which he received a commission and then completed navigator training, receiving his wings in October 1972. He served as a B-52H navigator in the SAC 46th Bomb Squadron, Grand Forks AFB, North Dakota and then as an Electronic Engineer in the Minuteman Program Office, Detachment 16, Anaheim, California. He was assigned to the School of Engineering, Air Force Institute of Technology in January 1977 for graduate studies in Guidance and Control.

Permanent address: 2631 Everglade Drive
Miramar, Florida 33023

This thesis was typed by Wawokiya Ursula Lawrence

AD-A064 047 AIR FORCE INST OF TECH WRIGHT-PATTERSON AFB OHIO SCH--ETC F/G 17/7
ERROR MODEL VERIFICATION FOR A THREE AXIS LASER GYRO STRAPDOWN --ETC(U)
DEC 78 R S LAWRENCE

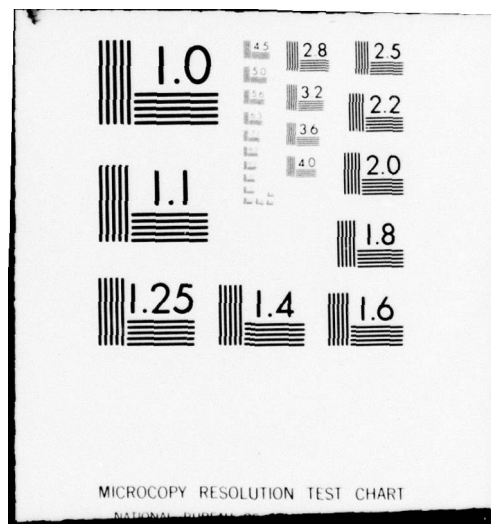
UNCLASSIFIED AFIT/GGC/EE/78-8

NL

20F2
AD
A064 047



END
DATE
FILMED
3-79
DDC



Unclassified

SECURITY CLASSIFICATION OF THIS PAGE (When Data Entered)

REPORT DOCUMENTATION PAGE		READ INSTRUCTIONS BEFORE COMPLETING FORM
1. REPORT NUMBER AFIT/GGC/EE/78-8	2. GOVT ACCESSION NO.	3. RECIPIENT'S CATALOG NUMBER -
4. TITLE (and Subtitle) ERROR MODEL VERIFICATION FOR A THREE AXIS LASER GYRO STRAPDOWN INERTIAL MEASUREMENT UNIT		5. TYPE OF REPORT & PERIOD COVERED MS Thesis
7. AUTHOR(s) Robert S. Lawrence Capt. USAF		6. PERFORMING ORG. REPORT NUMBER
9. PERFORMING ORGANIZATION NAME AND ADDRESS Air Force Institute of Technology (AFIT-EN) Wright-Patterson AFB, Ohio 45433		10. PROGRAM ELEMENT, PROJECT, TASK AREA & WORK UNIT NUMBERS
11. CONTROLLING OFFICE NAME AND ADDRESS Air Force Avionics Laboratory/RWA Wright-Patterson AFB OH 45433		12. REPORT DATE December, 1978
14. MONITORING AGENCY NAME & ADDRESS (if different from Controlling Office)		13. NUMBER OF PAGES 96
		15. SECURITY CLASS. (of this report) Unclassified
		15a. DECLASSIFICATION/DOWNGRADING SCHEDULE
16. DISTRIBUTION STATEMENT (of this Report) Approved for public release; distribution unlimited		
17. DISTRIBUTION STATEMENT (of the abstract entered in Block 20, if different from Report) Approved for public release; IAW AFR 190-17 Joseph P. Hipp, Major, USAF Director of Information 1-23-79		
18. SUPPLEMENTARY NOTES		
19. KEY WORDS (Continue on reverse side if necessary and identify by block number) Strapdown IMU Laser Gyroscopes		
20. ABSTRACT (Continue on reverse side if necessary and identify by block number) A digital data acquisition system was developed to obtain data from a Sperry laser gyroscope strapdown inertial measurement unit for error model verification. The system consisted of a laboratory test set-up with the inertial measurement unit (IMU) on the Genisco rate table and input/output interfaces such that meaningful IMU sensor data was recorded on magnetic tape with absence of a micro-processor. The recorded data was processed on the CDC 6600 digital computer by a specially developed program which formats the data		

Unclassified

SECURITY CLASSIFICATION OF THIS PAGE(When Data Entered)

in accordance to desired specifications. The calibration sequence for error model verification was a 6-position dynamic test for the laser gyros and a 6-position static test for the accelerometers. The result is a reliable and flexible system that can obtain data from the IMU in the laboratory for analysis.

Approved for public release
by [signature]

(A - 100) (b) (6) (A) (1) (b) (1) (c) (1) (d) (1) (e) (1) (f) (1) (g) (1) (h) (1) (i) (1) (j) (1) (k) (1) (l) (1) (m) (1) (n) (1) (o) (1) (p) (1) (q) (1) (r) (1) (s) (1) (t) (1) (u) (1) (v) (1) (w) (1) (x) (1) (y) (1) (z) (1)

Approved for public release
by [signature]

Unclassified

SECURITY CLASSIFICATION OF THIS PAGE(When Data Entered)